eLife

Reviewed Preprint
v2 • September 20, 2024
Revised by authors

Reviewed Preprint
v1 • November 1, 2023

Neuroscience

Deficiency of Orexin Receptor Type 1 in Dopaminergic Neurons Increases Novelty-Induced Locomotion and Exploration

Xing Xiao, Gagik Yeghiazaryan, Fynn Eggersmann, Anna L Cremer, Heiko Backes, Peter Kloppenburg, A Christine Hausen

Max Planck Institute for Metabolism Research, Department of Neuronal Control of Metabolism, Gleueler Strasse 50, 50931 Cologne, Germany • Excellence Cluster on Cellular Stress Responses in Aging Associated Diseases (CECAD) and Center for Molecular Medicine Cologne (CMMC), University of Cologne, Joseph-Stelzmann-Strasse 26, 50931 Cologne, Germany • Department of Biology, Institute for Zoology, University of Cologne, Zülpicher Strasse 47b, 50674 Cologne, Germany • Max Planck Institute for Metabolism Research, Multimodal Imaging of Brain Metabolism Group, Gleueler Strasse 50, 50931 Cologne, Germany

Abstract

Orexin signaling in the ventral tegmental area and substantia nigra promotes locomotion and reward processing, but it is not clear whether dopaminergic neurons directly mediate these effects. We show that dopaminergic neurons in these areas mainly express orexin receptor subtype 1 (Ox1R). In contrast, only a minor population in the medial ventral tegmental area express orexin receptor subtype 2 (Ox2R). To analyze the functional role of Ox1R signaling in dopaminergic neurons, we deleted Ox1R specifically in dopamine transporter-expressing neurons of mice and investigated the functional consequences. Deletion of Ox1R increased locomotor activity and exploration during exposure to novel environments or when intracerebroventricularely injected with orexin A. Spontaneous activity in home cages, anxiety, reward processing, and energy metabolism did not change. Positron emission tomography imaging revealed that Ox1R signaling in dopaminergic neurons affected distinct neural circuits depending on the stimulation mode. In line with an increase of neural activity in the lateral paragigantocellular nucleus (LPGi) of $Ox1R^{\Delta DAT}$ mice, we found that dopaminergic projections innervate the LPGi in regions where the inhibitory dopamine receptor subtype D2 but not the excitatory D1 subtype resides. These data suggest a crucial regulatory role of Ox1R signaling in dopaminergic neurons in novelty-induced locomotion and exploration.

eLife assessment

This manuscript describes **valuable** findings on the expression pattern of orexin receptors in the midbrain and how manipulating this system influences several behaviors, such as context-induced locomotor activity and exploration. The overall strength of evidence - which includes anatomical, viral manipulation studies, and brain imaging - is **solid** and broadly supports claims in the paper, however, there are several areas in which the conclusions are only partially supported by the statistical evidence. These results have implications for understanding the neural underpinnings of reward and will be of interest to neuroscientists and cognitive scientists with an interest in the neurobiology of reward.

https://doi.org/10.7554/eLife.91716.2.sa3

Introduction

Orexin neurons are exclusively located in the lateral hypothalamus (LH) and adjacent regions in the brain, including the perifornical area, and dorsomedial and posterior hypothalamus (Soya & Sakurai, 2020). Abundant orexin fibers innervate the ventral tegmental area (VTA) and substantia nigra (SN), which together contain the majority of dopaminergic neurons in humans and rodents (Fadel & Deutch, 2002; Hrabovszky et al., 2013; Peyron et al., 1998). There are also some dopaminergic neurons in other brain regions, although not all of these neurons express the dopamine transporter (DAT) (Koblinger et al., 2018; Sharples et al., 2014; Turiault et al., 2007). Both the orexin and dopaminergic systems control food intake, locomotor activity, reward processing as well as energy metabolism (Howe & Dombeck, 2016; Inutsuka & Yamanaka, 2013; Narayanan et al., 2010; Palmiter, 2007; Tsujino & Sakurai, 2013). Dopamine was discovered as a neuro-active molecule approximately 70 years ago and the dopaminergic system has diverse functions (Iversen & Iversen, 2007). In a simplified model the nigrostriatal dopaminergic system, containing the dopaminergic projections from SN to the dorsal striatum, predominantly regulates action selection and exploratory behaviors. In contrast, the mesolimbic and mesocortical dopaminergic systems, which consist of the dopaminergic pathways from the VTA to the ventral striatum and prefrontal cortex, predominantly regulate motivation, cognition, decision making, reward, and aversive behavior (Kutlu et al., 2021; Latif et al., 2021; Lerner et al., 2021; Roeper, 2013). Some VTA dopaminergic neurons also represent movements in trained animals (Lerner et al., 2021). Dopaminergic neurons modulate movement differently via direct and indirect pathways through the striatum (Kim et al., 2017; Kreitzer & Malenka, 2008; Roseberry et al., 2016). Co-release of other neuro-active molecules by dopaminergic terminals (Barcomb & Ford, 2023; Buck et al., 2021; Zych & Ford, 2022) and the spatial and temporal dynamics of dopamine release (Berke, 2018; Chantranupong et al., 2023; Liu et al., 2021) could further affect the precision and diversity of dopaminergic functions.

Orexin A injection into the VTA increases cocaine-and morphine-related reward processing (Mahler et al., 2012), and intra-SN injection of orexin A induces hyperlocomotion and stereotypic behaviors (Liu et al., 2018; Nakamura et al., 2000). On the other hand, systemic injection of dopamine receptor antagonists reduces orexin A-induced increase of hyperlocomotion, stereotypic and grooming behaviors (Nakamura et al., 2000). However, whether the above effects of orexin signaling in the VTA and SN are mediated by dopaminergic or non-dopaminergic cells is not yet clear.

The orexin system consists of the two peptides orexin A and B, which are derived from the precursor, prepro-orexin (de Lecea et al., 1998; Sakurai et al., 1998). Both are endogenous ligands for two G-protein-coupled receptors, orexin receptor subtype 1 (Ox1R), and 2 (Ox2R) (Sakurai et al., 1998). Orexin A activates both receptors, while orexin B predominantly activates Ox2R (Sakurai et al., 1998). The mRNA detection by *in situ* hybridization revealed the expression of both receptors in the VTA and SN (Marcus et al., 2001). However, the cell-type specific expression of Ox1R and Ox2R in the VTA and SN is not well understood. Electrophysiological studies showed that orexin receptors are present in dopaminergic VTA neurons (Baimel et al., 2017; Korotkova et al., 2003; Tung et al., 2016), whereas data for the SN seem controversial (Korotkova et al., 2002; Liu et al., 2018).

Here, we aim to map the expression patterns of Ox1R and Ox2R in dopaminergic VTA and SN neurons and investigate the functional role of Ox1R using conditional knockout mice.

Results

Ox1R is the predominant orexin receptor in dopaminergic neurons

To analyze the expression patterns of orexin receptors in dopaminergic VTA and SN neurons, we performed fluorescent *in situ* hybridization (RNAscope) of tyrosine hydroxylase (*Th*), Ox1R (*Hcrtr1*) and Ox2R (*Hcrtr2*) in control (Ox1R flox/flox, DAT wt/wt) mice and $Ox1R^{\Delta DAT}$ (Ox1R fl/fl, DAT-Cre tg/wt) mice, from the same breeding crossing mice carrying a loxP-flanked Ox1R-allele (Ox1R fl/fl) with DAT-Cre mice (Ekstrand et al., 2007).

In control mice, Ox1R was expressed in 44 -58% of dopaminergic neurons in all VTA and SN sub-regions, including the interfascicular (IF), paranigral (PN), parainterfascicular (PIF) and parabrachial (PBP) subnuclei of the VTA and SN. In contrast, Ox2R-positive dopaminergic neurons were mainly located in the medial VTA, including IF, PN, and PIF, with 25 - 42% of dopaminergic neurons expressing the Ox2R (**Figure 1A, C, D, G-I**; Figure 1—figure supplement 1A). While the above data were calculated as the mean percentages in the investigated mice, we also calculated the mean dopaminergic neuron numbers separately for those expressing both or exclusively one of the orexin receptor types. Thus, we could analyze the distribution of Ox1R-, Ox2R-, Ox1R and Ox2R-, and none (of orexin receptors)-expressing dopaminergic neurons in each VTA subregion and the SN (**Figure 1J**). The results were similar to the above: 47 - 59% of dopaminergic neurons expressed Ox1R in all VTA and SN sub-regions, and Ox2R was mainly expressed by 26 - 41% of dopaminergic neurons in the medial VTA (**Figure 1J**). 19 - 25% of dopaminergic neurons in the medial VTA expressed both Ox1R and Ox2R (**Figure 1J**). Of note, abundant Ox1R and Ox2R expression was present in Th-negative neurons in the VTA, SN, and neighboring regions (**Figure 1A, C, D**, Figure 1—figure supplement 1A).

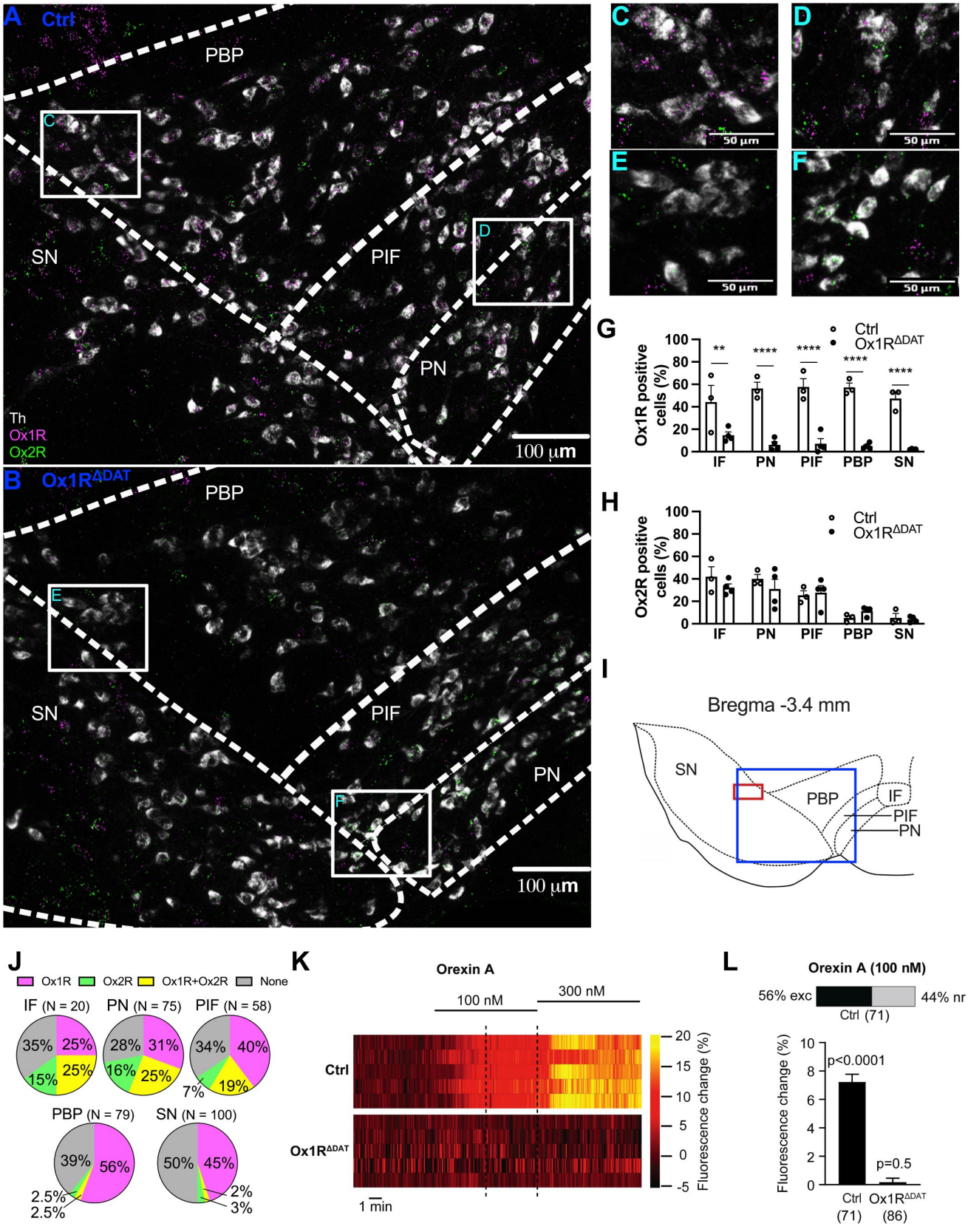
A Ctrl
PBP
SN
PIF
PN
Th
Ox1R
Ox2R
100 μm
B Ox1R^ΔDAT
C
D
E
F
50 μm
G
Ox1R positive cells (%)
Ctrl
Ox1R^ΔDAT
IF
PN
PIF
PBP
SN
H
Ox2R positive cells (%)
I
Bregma -3.4 mm
J
Ox1R
Ox2R
Ox1R+Ox2R
None
IF (N = 20)
PN (N = 75)
PIF (N = 58)
PBP (N = 79)
SN (N = 100)
K
Orexin A
100 nM
300 nM
Ctrl
Ox1R^ΔDAT
1 min
Fluorescence change (%)
L
Orexin A (100 nM)
56% exc
44% nr
Ctrl (71)
p<0.0001
p=0.5
Ctrl (71)
Ox1R^ΔDAT (86)

Figure 1

with 3 supplements. Ox1R predominantly mediates orexin-induced activation of dopaminergic neurons in the substantia nigra (SN).

Representative images of RNAscope *in situ* hybridization in SN and paranigral (PN), parainterfascicular (PIF) and parabrachial (PBP) subnuclei of the ventral tegmental area (VTA), of **(A)** a control and **(B)** an $Ox1R^{\Delta DAT}$ mouse. Amplifications of the **(C)** left and **(D)** right marked areas in white squares in (A). Amplifications of the **(E)** left and **(F)** right marked area in white squares in (B). White, tyrosine hydroxylase (Th); magenta, Ox1R; green, Ox2R. Scale bar: 100 µm (A, B) or 50 µm (C-F). Representative images of an overview in SN and VTA were shown in figure 1—figure supplement 1. Percentages of **(G)** Ox1R and **(H)** Ox2R positive neurons in Th positive neurons. IF, interfascicular subnuclei of VTA. Control, n = 3; $Ox1R^{\Delta DAT}$, n = 4. Data are represented as means ± SEM. **p < 0.01; ****p < 0.0001; as determined by two-way ANOVA followed by Sidak's post hoc test. **(I)** Schematic illustration showing the subnuclei of the left VTA and SN. The blue frame indicates the region where panel (A) and (B) are showing and the red frame indicates the region where calcium imaging was performed. **(J)** Pie charts showing Ox1R and Ox2R expression in dopaminergic neurons in the VTA and SN. 3 control mice were analyzed and N indicates the mean dopaminergic neuron numbers in the respective subregions. Magenta, dopaminergic neurons only expressing Ox1R; green, dopaminergic neurons only expressing Ox2R; yellow, dopaminergic neurons expressing both Ox1R and Ox2R; grey, dopaminergic neurons expressing neither Ox1R or Ox2R. **(K, L)** Effect of orexin A on dopaminergic SN neurons analyzed by Ca^{2+} imaging with GCaMP6. Recordings were performed in acute brain slices from control and $Ox1R^{\Delta DAT}$ male mice with GCaMP6 expressed in dopaminergic SN neurons. **(K)** Heat maps of 5 individual dopaminergic SN neurons from control (top) and 5 not orexin A-responsive dopaminergic SN neurons of $Ox1R^{\Delta DAT}$ mice (bottom). The recordings show the responses to 100 nM and 300 nM orexin A. The dashed lines indicate the range where the responses to 100 nM were quantified. **(L)** Top: The stacked bar shows the percentage of individual dopaminergic neurons in control mice in which the increase in $[Ca^{2+}]_i$ was larger than three times the standard deviation of the baseline fluorescence (3 σ criterion ≙ Z-score of 3), thus defining them as orexin A responsive (see Materials and Methods). None of the dopaminergic neurons in $Ox1R^{\Delta DAT}$ mice responded to orexin A. Bottom: Population Ca^{2+} responses upon 100 nM orexin A application from all recorded dopaminergic SN neurons of control and $Ox1R^{\Delta DAT}$ mice. Data are shown as the percentage of the maximal response to high K^+ saline. The significance of this mean response was tested for each group (control and $Ox1R^{\Delta DAT}$) using one-sample t-tests (control: p < 0.0001, n = 71; $Ox1R^{\Delta DAT}$: p = 0.5, n = 86). Bar graphs represent means ± SEM. p-values are provided above the bar graphs. n-values are given in brackets below the bar graphs.

Since most dopaminergic neurons express Ox1R, we focused the functional analysis on Ox1R signaling in dopaminergic neurons. Therefore, Ox1R was specifically inactivated in dopaminergic (DAT-expressing) neurons of mice ($Ox1R^{\Delta DAT}$). As a prerequisite for the functional analysis (behavior and PET imaging) validation of the Ox1R deletion was necessary. In $Ox1R^{\Delta DAT}$ mice, Ox1R expression was significantly reduced in dopaminergic neurons and remained unchanged in Th-negative cells (**Figure 1B, E-I**; Figure 1—figure supplement 1B). In contrast, the Ox2R expression patterns remained similar to that in the control mice, indicating the successful and specific knockout of Ox1R in dopaminergic neurons (**Figure 1B, E-I**; Figure 1—figure supplement 1B).

Next, we used perforated patch clamp recordings to establish that orexin A activates dopaminergic neurons not only in the mouse VTA (e.g., Baimel et al., 2017; Korotkova et al., 2003; Tung et al., 2016), but also in the mouse SN (Figure 1—figure supplement 2). In dopaminergic SN neurons that were pharmacologically isolated from GABAerigc and glutamatergic synaptic input 100 nM orexin increased the action potential frequency in 75% (6 of 8) of the neurons. Increasing the orexin A concentration to 300 nM further increased the firing frequency. This finding is consistent with previous extracellular recordings in rats (Liu et al. 2018). To also validate the Ox1R knockout in dopaminergic neurons functionally, we performed Ca^{2+} imaging in acute brain slices from control and $Ox1R^{\Delta DAT}$ mice. We used the genetically encoded Ca^{2+} indicator GCaMP6 to

monitor $[Ca^{2+}]_i$ specifically in dopaminergic (DAT-expressing) neurons. This analysis focused on dopaminergic neurons in the SN, which we used as an "indicator population" because a large number of these neurons express Ox1R. During the experiments, GABAergic and glutamatergic synaptic input was blocked. Bath-applied 100 nM orexin A markedly and significantly increased $[Ca^{2+}]_i$ in dopaminergic SN control neurons (**Figure 1I, K**, Figure 1—figure supplement 3). Increasing the orexin A concentration to 300 nM further increased $[Ca^{2+}]_i$ (**Figure 1I, K**, Figure 1—figure supplement 3). For quantification, we tested each neuron whether it responded to 100 nM orexin A. A neuron was considered orexin-responsive if the change in GCaMP fluorescence induced by orexin A was three times larger than the baseline fluorescence's standard deviation (3 σ criterion ≙ Z-score of 3). We found that 56% of the neurons tested responded to orexin A, while 44% of the neurons did not respond to orexin A (**Figure 1L**). These data are in very good agreement with the number of Ox1R-expressing neurons (**Figure 1J**). To determine the "population response" of all analyzed neurons, we measured the orexin-induced GCaMP6 fluorescence of each neuron expressed as a percentage of the GCaMP6 fluorescence induced by applying high (40 mM) K^+ saline (**Figure 1K**, Figure 1—figure supplement 3). This is a solid reference point since it reflects the GCaMP6 fluorescence at maximal voltage-activated Ca^{2+} influx. The "population response" of all analyzed neurons was expressed as the mean ± SEM of these responses (**Figure 1L**). The significance of this mean response was tested for each group (control and $Ox1R^{\Delta DAT}$) using a one-sample t-test. We found a highly significant and marked response of control neurons to 100 nM orexin A, while the Ox1R knockout neurons did not respond (control: $p < 0.0001$, $n = 71$; $Ox1R^{\Delta DAT}$: $p = 0.5$, $n = 86$; one sample t-test for each group) (**Figure 1L**).

In conclusion, Ox1R is the main orexin receptor expressed in dopaminergic VTA and SN neurons and mediates their activation by orexin. Therefore, we wanted to determine further the functional role of Ox1R signaling in dopaminergic neurons. By comparing control and $Ox1R^{\Delta DAT}$ mouse data, we first identified behaviors modulated by orexin via dopaminergic neurons. In a second step, we used PET imaging to define and map neuronal pathways modulated by orexin.

Ox1R in dopaminergic neurons regulates novelty-induced locomotion and exploration

The behavioral test included an analysis of locomotor behavior, novelty exploration, reward processing, anxiety, and energy homeostasis. Since sex differences exist in orexin-and dopamine-mediated behaviors (Durairaja & Fendt, 2020; Freeman et al., 2021; Lippert et al., 2020; Zachry et al., 2021), we analyzed behavioral phenotypes in both males and females. Compared to controls, $Ox1R^{\Delta DAT}$ mice did not show significant changes in spontaneous locomotor activity in home cages (Figure 2—figure supplement 1). When exposed to a novel open field, male and female $Ox1R^{\Delta DAT}$ mice exhibited an increase in locomotion and exploration, with increased traveling distance, ambulating time, and vertical activity in the open field test (**Figure 2A-C, E-G**). Female $Ox1R^{\Delta DAT}$ mice also showed increased stereotypic activity (**Figure 2D, H**). Furthermore, intracerebroventricular (ICV) injection of orexin A (1 nmol) induced a more pronounced increase of locomotor activity in both female and male $Ox1R^{\Delta DAT}$ mice, compared to control mice (**Figure 2I-L**).

In a hole-board test, female $Ox1R^{\Delta DAT}$ mice showed increased nose pokes into the holes in early (1st and 2nd) sessions compared to control mice (Figure 2—figure supplement 2B). This effect disappeared later when mice became familiar with the environment (3rd – 8th session) (Figure 2—figure supplement 2B). In the novel object recognition test, female $Ox1R^{\Delta DAT}$ mice spent more time with each of the two identical objects in an open field compared to control mice (Figure 2—figure supplement 2E). One hour later, when female mice were exposed to the same environment except that one object was replaced by a novel object, there was no significant difference between control and $Ox1R^{\Delta DAT}$ mice in exploring the novel object (Figure 2—figure supplement 2F). In contrast, male $Ox1R^{\Delta DAT}$ mice did not behave differently in the hole-board and novel object recognition

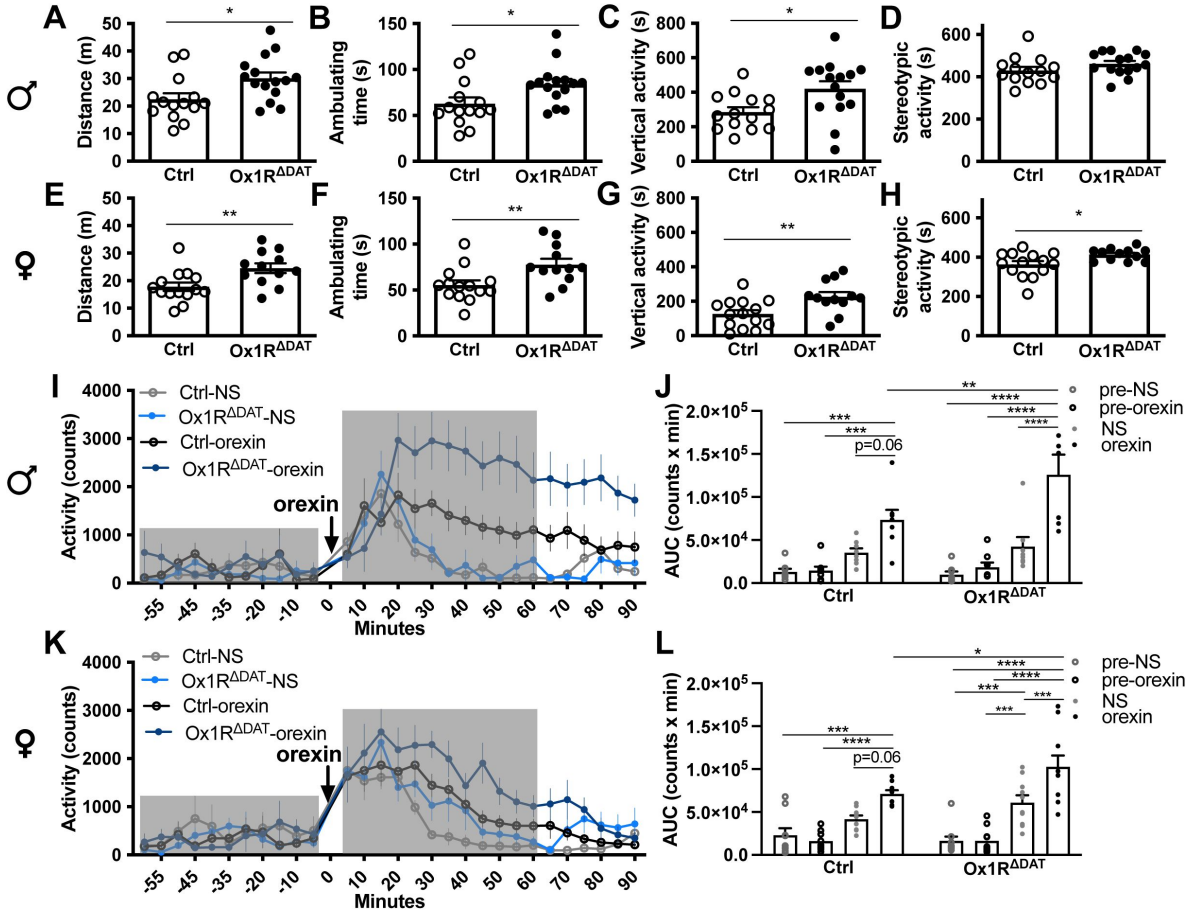

Figure 2

with 5 supplements. Deficiency of Ox1R in dopaminergic neurons increases locomotion and exploration behaviors.

(A) Total traveling distance, **(B)** ambulating time, **(C)** vertical activity and **(D)** stereotypic activity of male mice in the open field test. Control, n = 14; Ox1R$^{\Delta DAT}$, n = 15. **(E)** Total traveling distance, **(F)** ambulating time, **(G)** vertical activity and **(H)** stereotypic activity of female mice in the open field test. Control, n = 14; Ox1R$^{\Delta DAT}$, n = 12. Locomotor activity upon intracerebroventricular (ICV) injection of saline (NS) or orexin A in **(I)** male and **(K)** female control and Ox1R$^{\Delta DAT}$ mice. Grey boxes indicate the pre-and post-injection period for the area under curve (AUC) quantification. **(J, L)** Quantification of AUC pre-and post-saline and orexin A injection to (J) male and (L) female mice. Male (control and Ox1R$^{\Delta DAT}$), n = 8; female-control, n = 9; female-Ox1R$^{\Delta DAT}$, n = 10. Data are represented as means ± SEM. *p < 0.05; **p < 0.01; ***p < 0.001; ****p < 0.0001; as determined by unpaired two-tailed Student's t-test (A-C, E-H), or mixed two-way ANOVA followed by Sidak's post hoc test (J, L).

tests from controls (Figure 2—figure supplement 2A, C, D). This indicates that Ox1R signaling in dopaminergic neurons is more important for females in novelty-induced exploration, which was independent of novel object discrimination.

The behavioral changes seemed not related to alterations in anxiety since there were no detectable changes in anxiety-related behaviors, including the time spent in and the times of entries into the center area, light side and the open arms in an open field test, dark/light box test and 0-maze test, respectively (Figure 2—figure supplement 3).

Ox1R deletion in dopaminergic neurons did not change energy metabolism and reward processing

The orexin and dopaminergic systems are well known to regulate energy metabolism and reward processing (Howe & Dombeck, 2016; Inutsuka & Yamanaka, 2013; Narayanan et al., 2010; Palmiter, 2007; Tsujino & Sakurai, 2013). Therefore, we measured the impact of Ox1R deletion in dopaminergic neurons on metabolism and reward-related behaviors.

In the two-bottle preference test, mice have free access to both water and sweet solution (sucrose solution or the non-caloric sweetener, sucralose solution). In both of the control and $Ox1R^{\Delta DAT}$ groups, the percentages of sweet solution consumption in the total drinking were higher than 50%, indicating the preference of sweet solution (Figure 2—figure supplement 4A, D). The sucrose preference was more obvious for 1% and 2% than 0.5% sucrose solution (Figure 2—figure supplement 4B, E). There was no significant difference between the two groups (Figure 2—figure supplement 4A, B, D, E).

For the conditional place preference test (CPP, cocaine- vs. saline-injection-paired compartment), CPP score was calculated to show how much cocaine injection changed the time that mice spent in the compartment. Both of the control and $Ox1R^{\Delta DAT}$ groups showed a preference for cocaine injection without a significant difference between the two groups (Figure 2—figure supplement 4C, F).

In addition, neither male nor female $Ox1R^{\Delta DAT}$ mice showed significant changes in energy metabolism, including body weight, fat mass, respiratory exchanging ratio, energy expenditure, daily food intake, glucose tolerance and insulin sensitivity (Figure 2—figure supplement 5).

Ox1R in dopaminergic neurons regulates specific neural pathways under different conditions

To explore and map the underlying neuronal pathways of the orexin-mediated behaviors unbiasedly, we performed positron emission tomography (PET) imaging of control and $Ox1R^{\Delta DAT}$ mice upon ICV injection of orexin A or saline (control).

In $Ox1R^{\Delta DAT}$ mice under control conditions (saline injection), we observed higher neuronal activity around the medial preoptic area (MPA), piriform cortex (Pir), endopiriform claustrum, lateral stripe of the striatum (LSS), ventral part of subcoeruleus nucleus (SubCV), spinal trigeminal nucleus, spinal trigeminal tract (sp5), the intermediate reticular zone (IRt) and the gigantocellular reticular nucleus (Gi) than control mice (**Figure 3A**, Figure 3—figure supplement 1A and 2). Compared to control mice, central application of orexin A (1 nmol, ICV) to $Ox1R^{\Delta DAT}$ mice induced higher neuronal activity around the lateral paragigantocellular nucleus (LPGi), nucleus of the horizontal limb of the diagonal band (HDB) and magnocellular preoptic nucleus (MCPO), and lower activity around secondary motor cortex (M2), the dorsal bed nucleus of the stria terminalis (BNST), the hindlimb, shoulder, and trunk regions and barrel field of primary somatosensory cortex (S1HL, S1Sh, S1Tr, and S1BF), the lateral area of secondary visual cortex (V2L), primary

visual cortex (V1), Pir and dorsal endopiriform claustrum (DEn) (**Figure 3B**, Figure 3—figure supplement 1B and 2). PET imaging did not reveal significant changes in the VTA and SN (**Figure 3**, Figure 3—figure supplement 1).

Postmortem analysis of c-Fos staining revealed low c-Fos expression in dopaminergic neurons in the VTA and SN of $Ox1R^{\Delta DAT}$ and control mice after ICV injection of saline or orexin A (1 nmol). No apparent changes were observed among the groups. In contrast, clear orexin-induced c-Fos activity was observed in non-dopaminergic cells (Figure 3—figure supplement 3). This could affect the interpretation of dopaminergic contribution to behavioral effects in studies using ICV or intra-VTA/SN injection of orexin. Further studies would be needed to investigate how orexin directly and indirectly affect the VTA and SN neurons.

Dopamine receptors in the dorsal BNST and LPGi

Based on the PET imaging and behavioral findings, we further focused on the dorsal BNST and LPGi. They play a key functional role in regulating emotion, exploratory behaviors and locomotor speed, which are related to novelty-induced locomotion (Arber & Costa, 2022; Avery et al., 2016; Capelli et al., 2017; Crestani et al., 2013; Giardino et al., 2018; Takatoh et al., 2013). A schematic illustration of these analyzed brain areas is shown in Figure 4—figure supplement 1. We analyzed the dopaminergic pathways into the dorsal BNST and LPGi that could have been affected by the Ox1R. To this end, we injected Cre-dependent AAV-EYFP bilaterally into the VTA and SN of DAT-Cre (DAT^{EYFP}) and $Ox1R^{\Delta DAT}$ ($DAT^{\Delta Ox1R;\ EYFP}$) mice, and discovered dopaminergic projections in the dorsal BNST and LPGi (Figure 4—figure supplement 2), suggesting that VTA and SN dopaminergic neurons could directly modulate neuronal activity in the dorsal BNST and LPGi. To further explore this idea, we assessed the expression of Fos and dopamine receptors in the dorsal BNST and LPGi by immunostaining and RNAscope experiments.

Orexin A injection (1 nmol, ICV) induced higher c-Fos expression levels in LPGi of male $Ox1R^{\Delta DAT}$ mice compared to control mice (**Figure 4A, C**). Only the inhibitory D2 but not excitatory D1 subtypes of dopamine receptors (DRD2, DRD1) could be detected in LPGi (**Figure 4D, E**). Both receptors were detected around the lateral ventricle (as positive control), whereas no signal was detectable in LPGi incubated with a negative control probe for mice (**Figure 4F, G**). Th-positive fibers were detected in LPGi but not Gi (**Figure 4A, B**), consistent with previous reports (Kitahama et al., 2000). These data provides the anatomical basis for the possibility that Ox1R deletion in dopaminergic neurons results in the disinhibition of neural activity in LPGi via dopaminergic pathways.

Orexin A injection increased c-Fos expression in the dorsal BNST in control but not in $Ox1R^{\Delta DAT}$ mice (**Figure 4H, J**). The expression of DRD1 was significantly reduced, and DRD2 expression levels showed a tendency towards a decrease in dorsal BNST of $Ox1R^{\Delta DAT}$ mice (**Figure 4K-M**, Figure 4—figure supplement 3). The Th expression levels were not changed between genotypes (**Figure 4H, I**, Figure 4—figure supplement 3). This indicates that the dorsal BNST could be less activated due to the decrease of DRD1 and the lack of orexin-mediated activation of dopaminergic neurons.

Discussion

This study's behavioral experiments provide important evidence that Ox1R deficiency in DAT-expressing neurons leads to an increase in novelty-induced locomotion and exploration without altering energy metabolism and anxiety-or reward-processing-related behaviors. We found that Ox1R is the main subtype of orexin receptors in midbrain DAT-expressing neurons. The essential prerequisites for these functional studies were RNAscope and *ex vivo* Ca^{2+} imaging experiments, which confirmed the successful knockout of Ox1R in dopaminergic neurons. Further PET imaging,

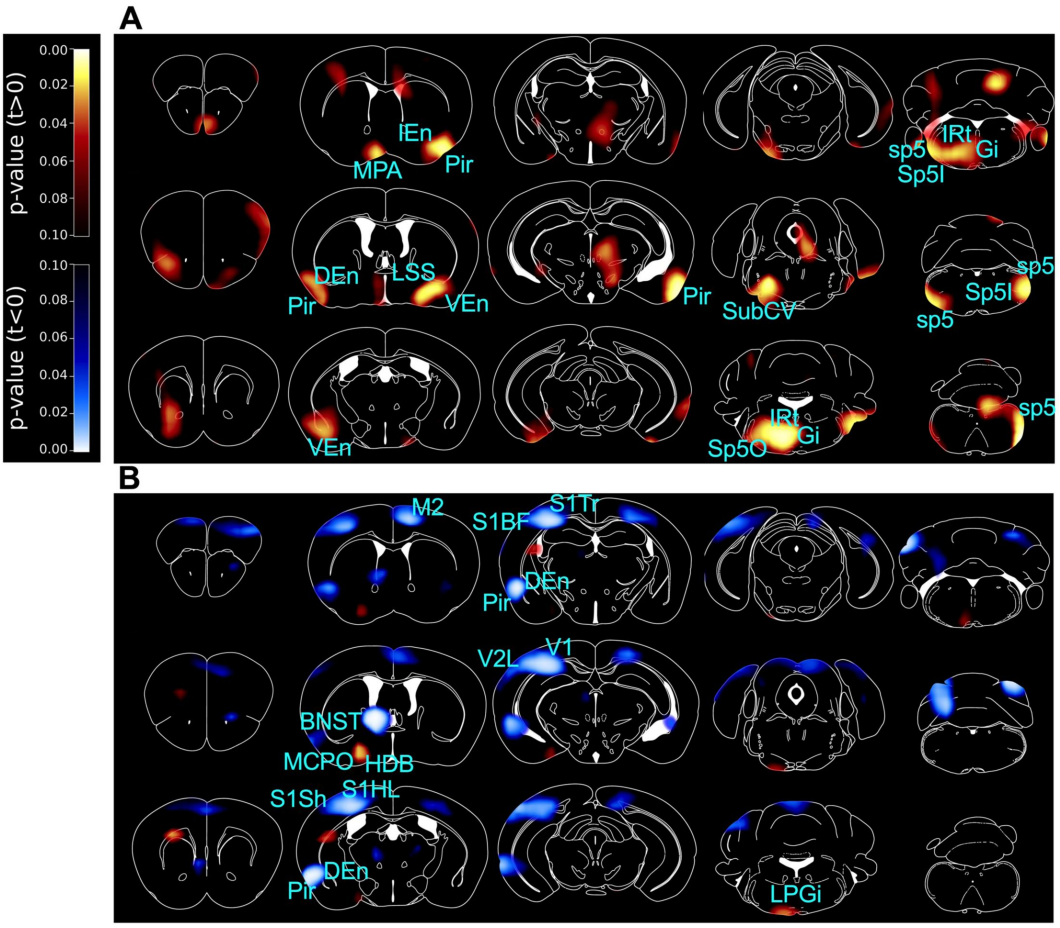

Figure 3

with 3 supplements. PET imaging studies comparing Ox1R$^{\Delta DAT}$ and control mice.

3D maps of p-values in PET imaging studies comparing Ox1R$^{\Delta DAT}$ and control mice, after intracerebroventricular (ICV) injection of **(A)** saline (NS) and **(B)** orexin A. Brain areas with significant changes are indicated. Control-NS, n = 8; control-orexin, n = 6; Ox1R$^{\Delta DAT}$ (NS and orexin), n = 8. Data are compared by unpaired two-tailed Student's t-test. M2, secondary motor cortex; MPA, medial preoptic area; Pir, piriform cortex; IEn, intermediate endopiriform claustrum; DEn, dorsal endopiriform claustrum; VEn, ventral endopiriform claustrum; LSS, lateral stripe of the striatum; BNST, the dorsal bed nucleus of the stria terminalis; HDB, nucleus of the horizontal limb of the diagonal band; MCPO, magnocellular preoptic nucleus; S1Sh, primary somatosensory cortex, shoulder region; S1HL, primary somatosensory cortex, hindlimb region; S1BF, primary somatosensory cortex, barrel field; S1Tr, primary somatosensory cortex, trunk region; V1, primary visual cortex; V2L, secondary visual cortex, lateral area; SubCV, subcoeruleus nucleus, ventral part; Gi, gigantocellular reticular nucleus; IRt, intermediate reticular nucleus; LPGi, lateral paragigantocellular nucleus; Sp5O, spinal trigeminal nucleus, oral part; Sp5I, spinal trigeminal nucleus, interpolar part; sp5, spinal trigeminal tract.

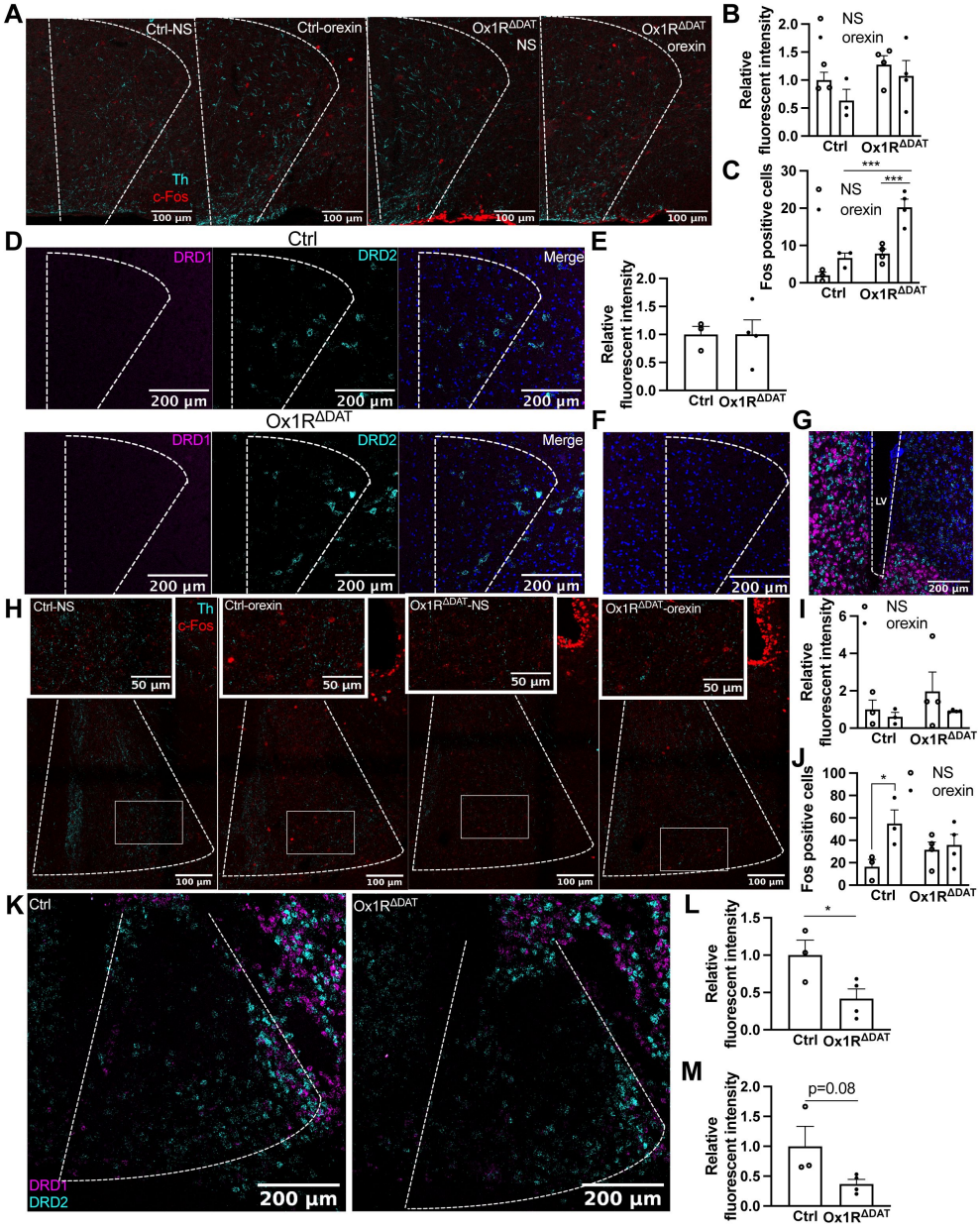

Figure 4

with 3 supplements. c-Fos and dopamine receptors in the lateral paragigantocellular nucleus (LPGi) and the dorsal bed nucleus of the stria terminalis (BNST).

(A) Representative images of c-Fos and tyrosine hydroxylase (Th) staining in LPGi of control and Ox1R$^{\Delta DAT}$ mice injected (ICV) with saline (NS) and orexin A. Quantification of **(B)** Th fluorescence and **(C)** c-Fos positive neurons in LPGi. **(D)** Representative images of D1 and D2 subtypes of dopamine receptor (DRD1 and DRD2) in LPGi of control and Ox1R$^{\Delta DAT}$ mice. **(E)** Quantification of DRD2 fluorescence in LPGi. **(F)** Representative images of a negative control staining of DRD1 and DRD2 in LPGi of control mice, and **(G)** a positive control staining around the lateral ventricle (LV). **(H)** Representative images of c-Fos and Th staining in the dorsal BNST of control and Ox1R$^{\Delta DAT}$ mice injected (ICV) with saline or orexin A. Quantification of **(I)** Th fluorescence and **(J)** c-Fos positive neurons in dorsal BNST. **(K)** Representative images of DRD1 and DRD2 in the dorsal BNST of control and Ox1R$^{\Delta DAT}$ mice. In the interest of clarity, the representative images for single channel signal are shown in the Figure 4—figure supplement 3. Quantification of **(L)** DRD1 and **(M)** DRD2 fluorescence in dorsal BNST. Scale bar: 200 µm (D, F, G, K), 100 µm (A, H) or 50 µm (insertions in H). Control, n = 3; Ox1R$^{\Delta DAT}$, n = 4. Cyan, Th; red, c-Fos (A, H). Magenta, DRD1; cyan, DRD2; blue, dapi (D, F, G, K). Data are represented as means ± SEM. *p < 0.05; ***p < 0.001; as determined by unpaired two-tailed Student's t-test (L, M), or two-way ANOVA followed by Sidak's post hoc test (C, J).

along with c-Fos and DRD expression analyses, provided initial insights into the underlying mechanisms. These findings can serve as a basis for developing testable working hypotheses on the systemic physiological role of orexin signaling.

Earlier studies showed orexin-induced activation of VTA dopaminergic neurons (Baimel et al., 2017; Korotkova et al., 2003; Tung et al., 2016). Whole-cell patch clamp recordings combined with mRNA measurement of the individually recorded VTA neurons revealed fewer Ox2R-than Ox1R-positive dopaminergic neurons (Korotkova et al., 2003), which is in line with our findings. While our electrophysiological and Ca^{2+} imaging data clearly show an orexin A-induced activation of dopaminergic SN neurons when GABAergic and glutamatergic synaptic input is blocked, previous *in vitro* (Korotkova et al., 2002) or *in vivo* extracellular electrophysiological recordings in rats (Liu et al., 2018) studies were controversial about whether orexin A could activate dopaminergic neurons in the SN. Since Ox1R and Ox2R are expressed by non-dopaminergic neurons around the SN, recordings in the absence of synaptic blockers, could detect a mixed direct and indirect orexin-induced response in dopaminergic neurons (Nair-Roberts et al., 2008). This may partially explain their controversial findings.

We found that Ox1R deficiency in dopaminergic neurons caused an increase in novelty-induced locomotion and exploration, which could indicate elevated arousal levels and hyperactivity. Interestingly, children with attention deficit and hyperactivity disorder (ADHD) have lower orexin A but unaltered orexin B levels in plasma compared to the healthy controls (Baykal et al., 2019). ADHD patients exhibit impaired dopaminergic functions, and medicine improving dopaminergic signaling is used to treat ADHD in clinics (Feldman & Reiff, 2014; Volkow & Swanson, 2013). Ox1R signaling in dopaminergic neurons is important to limit novelty-induced arousal and hyperactivity, which are related to task performance and learning capability. Novelty-induced behavioral response should be at proper levels under normal physiological conditions. The orexin-dopamine interaction blunting novelty-induced locomotion could be important to keep attention on the main task without being distracted too much by other random environmental stimuli. When this balance is disrupted, behavioral deficit may happen, such as ADHD.

We did not observe significant impact of Ox1R signaling in dopaminergic neurons on reward processing. Previous studies reported that Ox1R signaling in VTA promoted reward processing with pharmacological methods (Tsujino & Sakurai, 2013). The difference could have resulted from the involvement of non-dopaminergic neurons in VTA or different behavioral models. It would be interesting to identify the effect under other conditions, such as obesity and operant reward learning, in the future (Berke, 2018; Dabney et al., 2020; Kim et al., 2020; Wang et al., 2001).

The PET imaging results suggest that Ox1R signaling in dopaminergic neurons affects separate and distinct neuronal circuits, depending on the stimulation mode. Orexin and dopaminergic systems are known to increase arousal in mammals' sleep-wake transitions, locomotor activity, and motivation (Berke, 2018; Berridge et al., 2010; Furlong et al., 2009; Mahler et al., 2014). The orexin system responds to various environmental stimuli, such as stress and novelty (Berridge et al., 2010; Gonzalez et al., 2016). Projection-defined dopaminergic populations in the VTA exhibited different responses to orexin A (Baimel et al., 2017). Our PET imaging experiments, without orexin application, indicate that Ox1R signaling in dopaminergic neurons modulates brain regions (MPA, Pir, endopiriform claustrum, LSS, SubCV, spinal trigeminal nucleus, sp5, IRt and Gi) important for olfaction, eating, arousal and sleeping (Supplementary table 1).When central orexin levels were increased by orexin A injection, Ox1R signaling in dopaminergic neurons regulates HDB, MCPO, Pir, DEn, S1, V2L, V1, BNST, LPGi and M2, which are important for sensation, emotion, exploration, and action selection (Supplementary table 1). In future studies, it would be interesting to investigate the direct and indirect downstream pathways of Ox1R-expressing dopaminergic neurons. Interestingly, in the fruitfly *Drosophila melanogaster*, it has been shown that the dopaminergic system oppositely regulates sleep-wake arousal and environmentally

stimulated arousal, and the authors discussed the possibility to identify similar patterns in mammals (Lebestky et al., 2009). It was further suggested that the dopaminergic system differentially regulates arousal levels under different stimulating conditions (Lebestky et al., 2009; Lima & Miesenbock, 2005). Emotion perception affects the decision how to respond to the novelty. We think that novelty activates the orexin system, and Ox1R signaling in dopaminergic neurons promotes emotion perception and inhibits exploration.

DRD1 and DRD2 in the BNST regulate anxiety, fear, and addiction (De Bundel et al., 2016; Eiler et al., 2003; Giardino et al., 2018; Krawczyk et al., 2013). LGPi regulates exploratory behaviors and locomotor speed (Takatoh et al., 2013; Arber & Costa, 2022; Capelli et al., 2017). We found a potential direct impact of dopaminergic neurons on LPGi and BNST. The inhibitory D2 receptor was mainly expressed in LPGi, and the expression levels of the excitatory D1 receptor were decreased in BNST after Ox1R deletion in dopaminergic neurons. Our findings suggested that Ox1R deletion in dopaminergic neurons results in the disinhibition of neural activity in LPGi via dopaminergic pathways and the decrease of dopamine-mediated neural activity in BNST. It would be very interesting to further investigate these pathways in future. There are few publications on the functional relevance of dopaminergic projections in the LPGi. Future studies would be very interesting in terms of functionally analyzing DRD2 signaling in the LPGi and how orexin interacts with DRD2 signaling.

Materials and Methods

Animal care

All animal procedures were conducted in compliance with protocols approved by the local government authorities (Bezirksregierung Cologne, Germany) and were in accordance with National Institutes of Health guidelines. Mice were housed in groups of 3 -5 at 22°C - 24°C using a 12-hr light/12-hr dark cycle. Animals had *ad libitum* access to water and food at all times. Animals were fed a NCD (V1554, ssniff^{R}), which contains 67% calories from carbohydrates, 23% calories from protein, and 10% calories from fat.

Generation of Ox1R$^{\Delta DAT}$ mice

Mice carrying a loxP-flanked Ox1R-allele (Ox1R fl/fl) were generated in our facility (Xiao et al., 2021). Ox1R fl/fl mice were crossed with Dat-Cre mice (Ekstrand et al., 2007) to obtain Ox1R fl/fl, Dat-Cre tg/wt mice, i.e. dopaminergic-specific Ox1R knockout mice on a C57/Bl6 N background (Ox1R$^{\Delta DAT}$). Mice from the same breeding without the Cre transgene were used as controls (Ox1R fl/fl, Dat-Cre wt/wt).

Glucose and insulin tolerance tests

Glucose tolerance tests were performed on 12-weeks-old animals that had been fasted for 6 hours from 9 am. Insulin tolerance tests were performed on 11-weeks-old random-fed mice around 9 am. Animals received an intraperitoneal injection of 20% glucose (10 ml/kg body weight; KabiPac) or insulin (0.75 U/kg body weight; Sanofi-Aventis) into the peritoneal cavity, respectively. Blood glucose values were determined in whole venous blood using an automatic glucose monitor (Contour^{R}, Bayer). Glucose levels were determined in blood collected from the tail tip immediately before and 15, 30, and 60 minutes after the injection, with an additional value determined after 120 minutes for the glucose tolerance tests.

Analysis of body composition

Nuclear magnetic resonance (NMR) was employed to determine whole body composition of live animals on NCD at the age of 20 weeks using the NMR Analyzer minispec mq7.5 (Bruker Optik, Ettlingen, Germany).

Histology

Brains from male mice were removed, post-fixed in 4% paraformaldehyde (PFA) for the indicated time, and dehydrated in 20% sucrose in 0.1M phosphate-buffered saline (PBS) overnight. Brains were stored at -80°C until cutting.

Immunostaining

Brains were post-fixed for 6 h at 4 °C and cut (30 µm) with Leica CM3050 S Research Cryostat. Sections were incubated in 0.3% glycine for 10 min after washing in 0.1 M PBS for 2 × 10 min. After washing in PBS for another 10 min, sections were incubated in 0.03% SDS (in PBS) for 10 min before they got blocked with 3% donkey serum (in PBS, 0.25% Triton X-100) for 1 h at RT. Afterwards, they were incubated with primary antibodies, including goat anti-c-Fos (sc-526, Santa Cruz Biotechnology), chicken anti-GFP (ab13970, Abcam) and/or rabbit anti-Th (ab112, Abcam), for overnight (GFP) or 48 h (c-Fos and Th) at 4°C, washed in PBS for 3 × 10 min, and incubated with secondary antibodies, including Alexa Fluro 594 donkey anti-goat, FITC donkey anti-chicken, Alexa Fluro 488 donkey anti-rabbit (a11058, sa 1-7200 and a21206, Invitrogen), for 1 h at RT. After washing in PBS for 3 × 10 min, slices were mounted and covered with VECTASHIELD Antifade Mounting Medium with DAPI (Vector Laboratories). Slices were stained together at one time for each experiment to have identical conditions for comparable signals. Slides were stored at 4 °C until imaging. Images were obtained with confocal laser scanning microscope Leica TCS SP8.

RNAscope fluorescent in situ hybridization

Brains from 12-wk-old male mice were post-fixed for 20 - 22 h at RT and cut (20 µm). Slides were stored at -80°C until staining. All reagents were purchased from Advanced Cell Diagnostics, and the staining was performed with the RNAscope Multiplex Fluorescent v2 kit (ACD, Advanced Cell Diagnostics) according to the user manual. Probes for Ox1R (*Hcrtr1*, 471561-C3, ACD) and Ox2R (*Hcrtr2*, 471551, ACD), DRD1 (*Drd1a*, 406491-C2, ACD), DRD2 (*Drd2*, 406501), and Th (*Th*, 317621-C4) were purchased from ACD. In brief, slides were briefly washed in diethyl-pyrocarbonate (DEPC)-treated Millipore water, air dried, and then dried at 60°C overnight. On the second day, slides were treated with hydrogen peroxide (H_2O_2) for 10 min at RT, washed in water, and boiled in Target Retrieval solution (around 99.4 °C) for 8 -10 min. After a brief washing in water and dehydration in absolute ethanol, slides were incubated with protease IV for 30 min at RT. Slides were washed again in water and hybridized with the mixture of probes in different channels for 2 h in a humidified chamber at 40 °C. Afterwards, the hybridization was amplified with AMP 1 for 30 min, AMP 2 for 30 min and AMP 3 for 15 min. The signal was then developed for each channel. For example, for channel 1, slides were incubated with HRP-C1 for 15 min, the fluorophore for 30 min, and HRP blocker for 15 min. All amplification and development were performed at 40 °C, and 2 × 2 min of washing in ACD wash buffer was performed after each step. Finally, the slides were counterstained with DAPI for 1 min, mounted with Prolong™ Gold Antifade reagent with DAPI (Invitrogen), and covered with coverslips.

Slides were dried and stored at 4 °C. Imaging was performed with a confocal laser scanning microscope Leica TCS SP8.

Quantification

The images were manually analyzed with Image J/FIJI (version 1.50d). Dopaminergic cells were manually identified and outlined based on Th and DAPI signal. The integrated intensity of Ox1R and Ox2R signal in the delineated cells was automatically calculated by Image J. The integrated intensity in the negative control area was used as threshold, so that the cells with integrated intensity higher than the threshold were identified as Ox1R-or Ox2R-positive dopaminergic cells. c-Fos positive cell numbers were manually counted. Th, DRD1 and DRD2 fluorescence in the respective areas was taken as the integrated intensity automatically calculated by Image J.

Ca^{2+} imaging and electrophysiology

Animals and brain slice preparation

Perforated patch clamp recordings and Ca^{2+} imaging of dopaminergic SN neurons in acute brain slices were carried out essentially as described in Hess et al. (2023) and Xiao et al. (2021). Ca^{2+} imaging experiments were performed on brain slices from 18-19 week-old male control and $Ox1R^{\Delta DAT}$ mice. Animals were kept under standard laboratory conditions, with tap water and chow available ad libitum, on a 12h light/dark cycle. The animals were lightly anesthetized with isoflurane (B506; AbbVie Deutschland GmbH and Co KG) and decapitated. Coronal slices (280 µm) containing the SN were cut with a vibration microtome (VT1200 S; Leica) under cold (4°C), carbogenated (95% O_2 and 5% CO_2), glycerol-based modified artificial cerebrospinal fluid (GaCSF). GaCSF contained (in mM): 244 Glycerol, 2.5 KCl, 2 $MgCl_2$, 2 $CaCl_2$, 1.2 NaH_2PO_4, 10 HEPES, 21 $NaHCO_3$, and 5 Glucose adjusted to pH 7.2 with NaOH. Brain slices were transferred into carbogenated artificial cerebrospinal fluid (aCSF). First, they were kept for 20 min in a 35°C 'recovery bath' and then stored at room temperature (24°C) for at least 30 min before recording. During the recordings, the brain slices were continuously superfused with carbogenated aCSF at a flow rate of ~2.5 ml·min^{-1}. aCSF contained (in mM): 125 NaCl, 2.5 KCl, 2 $MgCl_2$, 2 $CaCl_2$, 1.2 NaH_2PO_4, 21 $NaHCO_3$, 10 HEPES, and 5 Glucose adjusted to pH 7.2 with NaOH. To block GABAergic and glutamatergic synaptic input, the aCSF contained 10^{-4} M PTX (picrotoxin, P1675; Sigma-Aldrich), 5 x 10^{-6} M CGP (CGP-54626 hydrochloride, BN0597, Biotrend), 5 x 10^{-5} M DL-AP5 (DL-2-amino-5-phosphonopentanoic acid, BN0086, Biotrend), and 10^{-5} M CNQX (6-cyano-7-nitroquinoxaline-2,3-dione, C127; Sigma-Aldrich). Orexin A (ab120212, Abcam) was bath-applied via the superfusion system at concentrations of 100 nM and 300 nM for 8 min for each concentration.

Perforated patch clamp recordings

Perforated patch clamp recordings were performed in current clamp mode. The experiments were carried out using protocols modified from previous studies, as summarized in Hess et al. (2023). SN dopaminergic neurons were identified according to their sag component / slow I_h-current (hyperpolarization-activated cyclic nucleotide-gated cation current), broad action potentials (Lacey et al., 1989; Neuhoff et al., 2002; Richards et al., 1997) and post hoc by biocytin-streptavidin labeling combined with TH-immunohistochemistry (Hess et al., 2013). The electrode solution contained (in mM): 140 K-gluconate, 10 KCl, 10 HEPES, 0.1 EGTA, 2 $MgCl_2$, and 1% biocytin (B4261, Sigma) adjusted to pH 7.2 with KOH. The calculated liquid junction potential between intracellular and extracellular solution was compensated. The patch electrode was tip-filled with electrode solution and backfilled with electrode solution, which contained the ionophore amphotericin B (A4888; Sigma) to achieve perforated patch recordings, 0.02% tetramethylrhodamine-dextran (3,000 MW, D3308, Invitrogen) to monitor the stability of the perforated membrane, and 1 % biocytin (B4261; Sigma-Aldrich) to label the recorded neuron. Amphotericin B was dissolved in

dimethyl sulfoxide (DMSO; D8418, Sigma) to a concentration of 200 µg*µl^{-1} and added to the electrode solution. The ionophore was added to the modified electrode solution shortly before use. The final concentration of amphotericin B was ~120-160 µg*ml^{-1}.

The orexin A (ab120212, Abcam) effect was analyzed by comparing the action potential frequencies measured during 4 min intervals recorded before and at the end of the peptide applications. To analyze the orexin A responsiveness, the neuron's firing rate averaged from 10 s intervals was taken as one data point. To determine the mean firing rate and standard deviation, 24 data points were averaged. On the single-cell level, a neuron was considered orexin-responsive if the change in firing induced by orexin A was three times larger than the standard deviation (3 σ criterion ≙ Z-score of 3). The significance of the mean response (Δfrequency) was tested using a one-sample Wilcoxon signed rank test. Data analysis was performed using Spike2 (version 7; Cambridge Electronic Design Ltd.), Igor Pro 6 (Wavemetrics), and Prism 8 (GraphPad Software Inc.).

Ca^{2+} imaging

All imaging experiments were performed on acute brain slices using the genetically encoded calcium indicator GCaMP6. At least 4 weeks were allowed for GCaMP6 virus expression. The imaging setup consisted of a Zeiss AxioCam/MRm CCD camera with a 1388x1040 chip and a Polychromator V (Till Photonics) that was coupled via an optical fiber into the Zeiss AxioExaminer upright microscope (Objective W "Plan-Apochromat" 20x/1.0 DIC D=0.17 M27 75mm). The camera and polychromator were controlled by the software Zen pro, including the module 'Physiology' (2012 blue edition, Zeiss). The SN neurons were identified according to their anatomical location and expression of the GCaMP6. Calcium signals in GCaMP6 expressing cells were monitored by images acquired at 470 nm excitation wavelengths with 20 ms exposure time at ~0.2 Hz. The emitted fluorescence was detected through a 500-550 nm bandpass filter (BP525/50), and data were acquired using 4x4 on-chip binning. Images were recorded in arbitrary units (AU) and analyzed as 16-bit grayscale images. Orexin A (ab120212, Abcam) in the concentrations of 100 nM and 300 nM was applied for 8 min each. To analyze the orexin effect, we compared the fluorescence measured in the cell bodies during 4 min intervals that were recorded immediately before and at the end of the peptide applications. This protocol was followed by applying high K^+ (40 mM) concentration saline (40 mM KCl; osmolarity adjusted by reducing the NaCl concentration) to identify cell bodies of neurons with functional GCaMP6 expression. Regions of interest (ROI) were defined after the experiment based on the high K^+ saline responses. The mean AU values of the ROIs were calculated in Image J. Time series analysis was performed with Igor Pro 6. To correct for bleaching artifacts, the baseline fluorescence (without orexin application) was fit. The extended fit was subtracted from the raw data. For each neuron, we tested whether it responded to orexin A. A neuron was considered orexin-responsive if the change in GCaMP fluorescence induced by orexin A was three times larger than the standard deviation (3 σ criterion ≙ Z-score of 3) of the baseline fluorescence. To determine the "population response" of all analyzed neurons, we measured the orexin-induced GCaMP6 fluorescence of each neuron expressed as a percentage of the GCaMP6 fluorescence induced by the high (40 mM) K^+ saline application. This is a solid reference point since it reflects the GCaMP6 fluorescence at maximal voltage-activated Ca^{2+} influx. The "population response" of all analyzed neurons was expressed as the mean ± SEM of these responses. The significance of this mean response was tested for each group (control and $Ox1R^{\Delta DAT}$) using a one-sample t-test. Image analysis was performed offline using Image J (version 1.53a), Igor Pro 6 (WaveMetrics), and Prism 8 (GraphPad Software Inc.).

Food intake and spontaneous activity

Mice (20 weeks old) were analyzed for food intake, spontaneous activity, respiratory exchanging ratio and energy expenditure in a PhenoMaster System (TSE Systems) as previously described (Jordan et al., 2011).

Behavioral studies

Mice were moved into the behavioral test room, weighed, and handled 1 week before the measurement. On the day of the tests, mice (9-15 weeks old) were moved near to the equipment and handled 1 h before the tests. There was a 1-week break between different behavioral tests for anxiety, exploration or locomotion when using the same mice.

Open field test (OFT), dark/light (D/L) box and Hole-board tests

OFT and D/L box tests were performed with a Seamless Open Field Starter Package for Mouse plus the Light/Dark Insert or the hole-board floor (Med Associates, Inc.) between 10 am to 4 pm.

To start OFT, mice were put in the middle of a clear Plexiglas® chamber (27.3 cm ξ 27.3 cm ξ 20.3 cm) sitting in a sound-attenuating cubicle, and mouse movement was automatically traced for 30 min with 48 infrared beams divided into the X, Y and Z plane. For the D/L box test, a black Plexiglas® box (half the size of the chamber) was inserted at the left side of the chamber, with an opening at the middle side. Mice were put in the middle of the light side and faced the openings. Mouse movement was traced for 5 min. For the hole-board test, a metal hole-board floor with 16 equally spaced holes for exploration was inserted in the chamber. Mice were put in the middle of the chambers and the nose pokes were monitored automatically for 10 min per session. There was 1 h break between each session. 4 sessions per day were analyzed for 2 consecutive days.

Elevated 0-maze test

An elevated 0-maze test was performed with TSE elevated 0-Maze in combination with the video tracking system TSE VideoMot 3D version 7.01. There are 2 closed and 2 open runways without a center position. The outer diameter is 48 cm, the arm width is 5 cm, the wall height is 10 cm and the base height is 55 cm. Mice were put in the middle of an open arm and faced to the closed arm to start the experiment. Mouse movement was monitored for 5 min.

Novel object recognition test

Novel object recognition test was modified from the publication before (Ruud et al., 2019). The mouse was acclimated and measured for 10 min in the 1st session and for 5 min in the 2nd session on the same day, in a polycarbonate box with non-transparent walls (50 cm ξ 50 cm ξ 30 cm). Two objects were present in the box. In the 1st session, two identical objects (glass beaker filled with blue marbles) were present and fixed with odor-free adhesive to the ground flooring at two sides of the box delineated diagonally. In each diagonal corner, the object is 11.5 cm and 14 cm from each wall respectively, and the distance between the two objects is 17.5 cm. Mice always started at the same corner which was between the two fixed objects and were allowed to explore and learn the experimental area and objects. In the 2nd session which started after a 1-h break in the home cage, one of the two identical objects was replaced with a novel object (Lego® Primo brick), and mice were allowed again to explore the environment and objects. The positions of the mouse nose, tail and center were monitored with a video tracking system TSE VideoMot 2. The interaction with a fixed object was identified when the nose was facing the object within a distance of 2 cm.

Conditioned place preference test for cocaine

The test was modified from previous publication (Ruud et al., 2019), and was performed in a polycarbonate box with non-transparent walls. The box was separated into 3 compartments with 2 independent partitions. It contains a left compartment with zebra stripes (white and black) painted on the wall and a rough ground (16.5 x 13.2 x 21.2 cm), a small middle area (7.0 x 13.2 x 21.2 cm), and a right compartment with a white wall and smooth ground. Mouse movement was monitored with TSE VideoMot 2 for 30 min per session, 1 session per day. Mice started from the middle area and had access to both left and right compartments through an opening (4.0 cm x 4.2

cm) in the partition during the habituation and pre-test days (d1-3) and on the test day (d10), and were put into and kept in either the left or right compartment without an opening in the partition during the conditioning phase (d4-9). The preference of the two compartments by nature was analyzed during the pre-test days. At the conditioning phase, on alternative days, mice received i.p. injection of cocaine (5 mg/kg BW) or saline immediately before entering the respective compartments. Cocaine and saline were always paired to the non-preferred and preferred compartments, which were determined by pre-tests, respectively. There was no injection on the habituation, pre-test or test days. The percentage of time spent in the reward-paired compartment was calculated: 100 x time spent in the compartment / (total time -time spent in the middle area). The CPP score was then analyzed using the calculated percentage of time: 100 x (time on the test day – time on pre-test days)/ time on pre-test days. The pre-test and test days were before and after the conditioning, respectively. Thus, the CPP score above zero indicates that the CPP preference is developed.

Sucrose/sucralose preference test

Two-bottle tests were performed with 2 15-ml falcon tubes connected to sippers. Mice were single caged 1 week before the beginning of the experiment. 2 falcon tubes filled with water (side-by-side) replaced the normal water bottle. Water intake was monitored for a week to make sure mice adjusted to drinking from the sippers. When the test started, 2 new sipper tubes of water were used for 2 days of baseline measurement and were then replaced with one containing water and one containing sucrose/sucralose solution for 2 days of preference measurement. Animals received a 0.5%, 1% and 2% (w/v) sucrose solution and 1 mM sucralose solution in sequential. Between the preference tests of different solutions, 2 days of baseline measurement were performed with 2 new sipper tubes of water as a washout. To avoid side bias, the positions of 2 sipper tubes were switched every day, with the sucrose/sucralose tube always starting on the non-preferred position, which was determined by water intake on the day before the preference measurement. Sipper tubes were weighed every day.

ICV cannula implantation and injection

12-wk-old mice received 1 mg/ml of tramadol in drinking water 2 d before the surgeries. On the day of surgery, mice were anesthetized with isoflurane, and a bolus of buprenorphine (0.1 mg/kg BW) was given (i. p.) to reduce pain. Brain regions were identified according to the atlas (Franklin & Paxinos, 2007). After alignment of the brain in the stereotaxic surgery platform, one small hole was drilled in the skull and the ICV cannula (26 gauge, Plastics One) was immediately implanted (AP: -0.2 mm, ML: +1 mm, DV: -2.4 mm) and fixed to the skull with dental acrylic (Super-Bond C&B). The dummy cannula caps were inserted to close and protect the cannula. Mice received a bolus of meloxicam (5 mg/kg BW, s.c.), and tramadol in drinking water for 3 d after surgeries to relieve pain. BW was checked twice a day. Experiments started at least 1 week later. For injection, the catheter was attached to an injector (Plastics One), which was inserted through the cannula. orexin A (Phoenix Pharmaceuticals) was injected slowly at the dose of 1 nmol dissolved in 2 ul of saline. Starting from 5 days before the injection, mice and the dummy cannula caps were handled for acclimation daily. The locomotion activity was measured in a PhenoMaster System (TSE Systems), and mice were acclimated to the system at least 5 days before the test.

PET imaging

PET imaging was performed using an Inveon preclinical PET/CT system (Siemens). Male mice were anesthetized with 2% isoflurane in 65%/35% nitrous oxide/oxygen gas, injected with saline or orexin A (Phoenix Pharmaceuticals) and positioned on a dedicated mouse carrier (MEDRES, Germany) carrying two mice. Body temperature was maintained at 37.0 ± 0.5°C by a thermostatically controlled water heating system. For injection of the radiotracer, a catheter consisting of a 30G cannula connected to a polythene tubing (ID = 0.28 mm) was inserted into the tail vein and fixated by a drop of glue. After starting the PET scan, 7-8 MBq of [18F]FDG in 50-100

µl saline were injected per mouse. Emission data were acquired for 45 minutes. Thereafter, animals were automatically moved into the CT gantry, and a CT scan was performed (180 projections/360°, 200 ms, 80 kV, 500 µA). The CT data were used for attenuation correction of the PET data, and the CT image of the scull was used for image co-registration. Plasma glucose levels were determined from a tail vein blood sample using a standard glucometer (Bayer) after removing the tail vein catheters. PET data were histogrammed in time frames of 12x30s, 3x60s, 3x120s, 7x240s, Fourier rebinned, and images were reconstructed using the MAP-SP algorithm provided by the manufacturer. For co-registration, the imaging analysis software Vinci was used (Cizek et al., 2004). Images were co-registered to a 3D mouse brain atlas constructed from the 2D mouse brain atlas published by Paxinos (Paxinos et al., 2013).

Kinetic modeling

An image-derived input function was extracted from the PET data of the aorta, which could be identified in the image of the first time frame of each animal. Input function data were corrected for partial volume effect by assuming a standardized volume fraction of 0.6 (Green et al., 1998). Parametric images of the [18F]FDG kinetic constants K_1, k_2, k_3, and k_4 were determined by a voxel-by-voxel (voxel size = 0.4 mm x 0.4 mm x 0.8 mm) fitting of data to a two-tissue-compartment kinetic model. K_1 is the constant for transport from blood to tissue, k_2 for transport from tissue to blood, k_3 the constant for phosphorylation of [18F]FDG to [18F]FDG-6-phosphate, and k_4 the constant for dephosphorylation. The ratio of tissue and plasma glucose concentrations (C_E/C_P) is a measure for glucose transport and is given by $C_E/C_P = K_1/(k_2 + k_3/0.26)$ (Backes et al., 2011; Jais et al., 2016). Since neuronal activation is accompanied by increased glucose transport and this parameter is less sensitive to changes in plasma glucose level, we use alterations of glucose transport (C_E/C_P) as surrogate for alterations in neuronal activation.

Statistics

Statistical testing was performed by application of a voxel-wise t-test between groups. 3D maps of p-values allow for the identification of regions with significant differences in the parameters. From these regions, we defined volumes of interest (VOIs) and performed additional statistical testing for these VOIs. For presentation only, 3D maps of p-values were re-calculated on a 0.1 mm x 0.1 mm x 0.1 mm grid from the original dataset using trilinear interpolation.

Virus injection

Male mice received 1 mg/ml of tramadol in drinking water 2 d before the surgeries. On the day of surgery, mice were anesthetized with isoflurane and a bolus of buprenorphine (0.1 mg/kg BW) was given (i. p.) to reduce pain. Brain regions were identified according to the atlas (Franklin & Paxinos, 2007). After alignment of the brain in the stereotaxic surgery platform, 1 or 4 small holes were drilled in the skull at specific coordinates. The virus, pAAV-Ef1a-DIO EYFP (~$1x10^{13}$ GC/ml, 300 nl, Addgene) was bilaterally injected into VTA and SN of 10 wk old mice, with micropipettes pulled in house with a heating system. The coordinates from Bregma were: anterior-posterior, AP: -3.4 mm; medial-lateral, ML: ±0.5/1.25 mm; dorsal-ventral, DV: -4.2 mm. The GCaMP6 virus (AAV1.Syn.Flex.GCaMP6s.WPRE.SV40, ~$4x10^{12}$ GC/ml, 300 nl, Penn Vector Core) was injected to left SN (AP: -3.4 mm, ML: 1.1 mm, DV: -4.2 mm) of 12 wk old mice, to specifically express GCaMP6 in dopaminergic neurons. After virus injection, mice received a bolus of meloxicam (5 mg/kg BW, s.c.), and tramadol in drinking water for 3 d after surgeries to relieve pain. BW was checked twice a day. Experiments started at least 4 weeks later than virus injection to allow virus expression.

Statistical methods

All numerical values are expressed as the mean ± SEM. Statistical analyses were conducted using GraphPad PRISM (version 8) unless stated otherwise. Datasets with only two independent groups were analyzed for statistical significance using an unpaired two-tailed Student's t-test. Datasets

subjected to two independent factors were analyzed using two-way ANOVA followed by Sidak's post hoc test. All p-values < 0.05 were considered significant (*p < 0.05, **p < 0.01, and ***p < 0.001, ****p < 0.0001).

Acknowledgements

We acknowledge Hella Brönneke for outstanding support, Jens Alber, Pia Scholl, Christiane Schäfer, Nadine Spenrath, Ina Stünkel, Kerstin Marohl, Antonia Lorenz and Helmut Wratil for outstanding technical assistance. We received funding by the DFG within the framework of the TRR 134 (A.C.H., P.K.), DFG-401832153 (P.K.) and within the Excellence Initiative by German Federal and State Governments (CECAD). This work was funded (in part) by the Helmholtz Alliance ICEMED (Imaging and Curing Environmental Metabolic Diseases) through the Initiative and Networking Fund of the Helmholtz Association. X.X. received funding from CECAD Family Support. G.Y. gratefully acknowledges financial doctoral support from the DFG-233886668/GRK1960.

Author Contributions

X.X. and A.C.H. conceived the project, designed the experiments, and wrote the manuscript with input from the other authors. A.C.H. generated the Ox1R flox mouse line. X.X. performed all the experiments apart from calcium imaging and electrophysiological recording experiments (G.Y., F.E. and P.K.) and PET imaging experiments (A.L.C. and H.B.). All authors discussed the data, commented on the manuscript before submission, and agreed with the final submitted manuscript.

Competing Interests

The authors declare no competing interests.

Data Availability

There are no restrictions on data availability.

References

Arber S., Costa R. M (2022) **Networking brainstem and basal ganglia circuits for movement** *Nat Rev Neurosci* **23**:342–360 https://doi.org/10.1038/s41583-022-00581-w

Avery S. N., Clauss J. A., Blackford J. U (2016) **The Human BNST: Functional Role in Anxiety and Addiction** *Neuropsychopharmacology* **41**:126–141 https://doi.org/10.1038/npp.2015.185

Backes H., Walberer M., Endepols H., Neumaier B., Graf R., Wienhard K., Mies G (2011) **Whiskers area as extracerebral reference tissue for quantification of rat brain metabolism using (18)F-FDG PET: application to focal cerebral ischemia** *Journal of Nuclear Medicine* **52**:1252–1260 https://doi.org/10.2967/jnumed.110.085266

Baimel C., Lau B. K., Qiao M., Borgland S. L (2017) **Projection-target-defined effects of orexin and dynorphin on VTA dopamine neurons** *Cell Rep* **18**:1346–1355 https://doi.org/10.1016/j.celrep.2017.01.030

Barcomb K., Ford C. P (2023) **Alterations in neurotransmitter co-release in Parkinson's disease** *Exp Neurol* **370** https://doi.org/10.1016/j.expneurol.2023.114562

Baykal S., Albayrak Y., Durankus F., Guzel S., Abbak O., Potas N., Beyazyuz M., Karabekiroglu K., Donma M. M (2019) **Decreased serum orexin A levels in drug-naive children with attention deficit and hyperactivity disorder** *Neurol Sci* **40**:593–602 https://doi.org/10.1007/s10072-018-3692-8

Berke J. D (2018) **What does dopamine mean?** *Nat Neurosci* **21**:787–793 https://doi.org/10.1038/s41593-018-0152-y

Berridge C. W., Espana R. A., Vittoz N. M (2010) **Hypocretin/orexin in arousal and stress** *Brain Res* **1314**:91–102 https://doi.org/10.1016/j.brainres.2009.09.019

Buck S. A., Torregrossa M. M., Logan R. W., Freyberg Z (2021) **Roles of dopamine and glutamate co-release in the nucleus accumbens in mediating the actions of drugs of abuse** *FEBS J* **288**:1462–1474 https://doi.org/10.1111/febs.15496

Capelli P., Pivetta C., Soledad Esposito M., Arber S (2017) **Locomotor speed control circuits in the caudal brainstem** *Nature* **551**:373–377 https://doi.org/10.1038/nature24064

Chantranupong L., Beron C. C., Zimmer J. A., Wen M. J., Wang W., Sabatini B. L (2023) **Dopamine and glutamate regulate striatal acetylcholine in decision-making** *Nature* **621**:577–585 https://doi.org/10.1038/s41586-023-06492-9

Cizek J., Herholz K., Vollmar S., Schrader R., Klein J., Heiss W. D (2004) **Fast and robust registration of PET and MR images of human brain** *Neuroimage* **22**:434–442 https://doi.org/10.1016/j.neuroimage.2004.01.016

Crestani C. C., Alves F. H., Gomes F. V., Resstel L. B., Correa F. M., Herman J. P (2013) **Mechanisms in the bed nucleus of the stria terminalis involved in control of autonomic and neuroendocrine functions: a review** *Curr Neuropharmacol* **11**:141–159 https://doi.org/10.2174/1570159X11311020002

Dabney W., Kurth-Nelson Z., Uchida N., Starkweather C. K., Hassabis D., Munos R., Botvinick M (2020) **A distributional code for value in dopamine-based reinforcement learning** *Nature* **577**:671–675 https://doi.org/10.1038/s41586-019-1924-6

De Bundel D., Zussy C., Espallergues J., Gerfen C. R., Girault J. A., Valjent E. (2016) **Dopamine D2 receptors gate generalization of conditioned threat responses through mTORC1 signaling in the extended amygdala** *Molecular Psychiatry* **21**:1545–1553 https://doi.org/10.1038/mp.2015.210

de Lecea L. *et al.* (1998) **The hypocretins: hypothalamus-specific peptides with neuroexcitatory activity** *Proc Natl Acad Sci U S A* **95**:322–327 https://doi.org/10.1073/pnas.95.1.322

Durairaja A., Fendt M (2020) **Orexin deficiency modulates cognitive flexibility in a sex-dependent manner. Genes Brain Behav** *e* **12707** https://doi.org/10.1111/gbb.12707

Eiler W. J, Seyoum R., Foster K. L., Mailey C., June H. L. (2003) **D1 dopamine receptor regulates alcohol-motivated behaviors in the bed nucleus of the stria terminalis in alcohol-preferring (P) rats** *Synapse* **48**:45–56 https://doi.org/10.1002/syn.10181

Ekstrand M. I. *et al.* (2007) **Progressive parkinsonism in mice with respiratory-chain-deficient dopamine neurons** *Proc Natl Acad Sci U S A* **104**:1325–1330 https://doi.org/10.1073/pnas.0605208103

Fadel J., Deutch A. Y (2002) **Anatomical substrates of orexin–dopamine interactions: lateral hypothalamic projections to the ventral tegmental area** *Neuroscience* **111**:379–387 https://doi.org/10.1016/S0306-4522(02)00017-9

Feldman H. M., Reiff M. I (2014) **Clinical practice. Attention deficit-hyperactivity disorder in children and adolescents** *N Engl J Med* **370**:838–846 https://doi.org/10.1056/NEJMcp1307215

Franklin K. B. J., Paxinos G. (2007) **The mouse brain in stereotaxic coordinates (3rd ed.)**

Freeman L. R., Bentzley B. S., James M. H., Aston-Jones G (2021) **Sex differences in demand for highly palatable foods: role of the orexin system** *Int J Neuropsychopharmacol* **24**:54–63 https://doi.org/10.1093/ijnp/pyaa040

Furlong T. M., Vianna D. M., Liu L., Carrive P (2009) **Hypocretin/orexin contributes to the expression of some but not all forms of stress and arousal** *Eur J Neurosci* **30**:1603–1614 https://doi.org/10.1111/j.1460-9568.2009.06952.x

Giardino W. J., Eban-Rothschild A., Christoffel D. J., Li S. B., Malenka R. C., de Lecea L. (2018) **Parallel circuits from the bed nuclei of stria terminalis to the lateral hypothalamus drive opposing emotional states** *Nat Neurosci* **21**:1084–1095 https://doi.org/10.1038/s41593-018-0198-x

Gonzalez J. A., Iordanidou P., Strom M., Adamantidis A., Burdakov D (2016) **Awake dynamics and brain-wide direct inputs of hypothalamic MCH and orexin networks** *Nat Commun* **7** https://doi.org/10.1038/ncomms11395

Green L. A., Gambhir S. S., Srinivasan A., Banerjee P. K., Hoh C. K., Cherry S. R., Sharfstein S., Barrio J. R., Herschman H. R., Phelps M. E (1998) **Noninvasive methods for quantitating blood time-activity curves from mouse PET images obtained with fluorine-18-fluorodeoxyglucose** *Journal of Nuclear Medicine* **39**:729–734

Hess M. E. *et al.* (2013) **The fat mass and obesity associated gene (Fto) regulates activity of the dopaminergic midbrain circuitry** *Nat Neurosci* **16**:1042–1048 https://doi.org/10.1038/nn.3449

Hess S., Wratil H., Kloppenburg P (2023) **Perforated Patch Clamp Recordings in ex vivo Brain Slices from Adult Mice** *Bio Protoc* **13** https://doi.org/10.21769/BioProtoc.4741

Howe M. W., Dombeck D. A (2016) **Rapid signalling in distinct dopaminergic axons during locomotion and reward** *Nature* **535**:505–510 https://doi.org/10.1038/nature18942

Hrabovszky E., Molnar C. S., Borsay B. A., Gergely P., Herczeg L., Liposits Z (2013) **Orexinergic input to dopaminergic neurons of the human ventral tegmental area** *PLoS One* **8** https://doi.org/10.1371/journal.pone.0083029

Inutsuka A., Yamanaka A (2013) **The physiological role of orexin/hypocretin neurons in the regulation of sleep/wakefulness and neuroendocrine functions** *Front Endocrinol (Lausanne* **4** https://doi.org/10.3389/fendo.2013.00018

Iversen S. D., Iversen L. L (2007) **Dopamine: 50 years in perspective** *Trends in Neurosciences* **30**:188–193 https://doi.org/10.1016/j.tins.2007.03.002

Jais A. *et al.* (2016) **Myeloid-cell-derived VEGF maintains brain glucose uptake and limits cognitive impairment in obesity** *Cell* **165**:882–895 https://doi.org/10.1016/j.cell.2016.03.033

Jordan S. D. *et al.* (2011) **Obesity-induced overexpression of miRNA-143 inhibits insulin-stimulated AKT activation and impairs glucose metabolism [Research Support** *Non-U.S. Gov't]. Nat Cell Biol* **13**:434–446 https://doi.org/10.1038/ncb2211

Kim H. F., Amita H., Hikosaka O (2017) **Indirect Pathway of Caudal Basal Ganglia for Rejection of Valueless Visual Objects** *Neuron* **94**:920–930 https://doi.org/10.1016/j.neuron.2017.04.033

Kim H. R. *et al.* (2020) **A Unified Framework for Dopamine Signals across Timescales** *Cell* **183**:1600–1616 https://doi.org/10.1016/j.cell.2020.11.013

Kitahama K., Nagatsu I., Geffard M., Maeda T (2000) **Distribution of dopamine-immunoreactive fibers in the rat brainstem** *Journal of Chemical Neuroanatomy* **18**:1–9 https://doi.org/10.1016/S0891-0618(99)00047-2

Koblinger K., Jean-Xavier C., Sharma S., Fuzesi T., Young L., Eaton S. E. A., Kwok C. H. T., Bains J. S., Whelan P. J (2018) **Optogenetic activation of A11 region increases motor activity** *Front Neural Circuits* **12** https://doi.org/10.3389/fncir.2018.00086

Korotkova T. M., Eriksson K. S., Haas H. L., Brown R. E (2002) **Selective excitation of GABAergic neurons in the substantia nigra of the rat by orexin/hypocretin in vitro** *Regul Pept* **104**:83–89 https://doi.org/10.1016/s0167-0115(01)00323-8

Korotkova T. M., Sergeeva O. A., Eriksson K. S., Haas H. L., Brown R. E (2003) **Excitation of ventral tegmental area dopaminergic and nondopaminergic neurons by orexins/hypocretins** *J Neurosci* **23**:7–11

Krawczyk M. *et al.* (2013) **D1 dopamine receptor-mediated LTP at GABA synapses encodes motivation to self-administer cocaine in rats** *Journal of Neuroscience* **33** https://doi.org/10.1523/Jneurosci.1784-13.2013

Kreitzer A. C., Malenka R. C (2008) **Striatal plasticity and basal ganglia circuit function** *Neuron* **60**:543–554 https://doi.org/10.1016/j.neuron.2008.11.005

Kutlu M. G., Zachry J. E., Melugin P. R., Cajigas S. A., Chevee M. F., Kelly S. J., Kutlu B., Tian L., Siciliano C. A., Calipari E. S (2021) **Dopamine release in the nucleus accumbens core signals perceived saliency** *Curr Biol* **31**:4748–4761 https://doi.org/10.1016/j.cub.2021.08.052

Lacey M. G., Mercuri N. B., North R. A (1989) **Two cell types in rat substantia nigra zona compacta distinguished by membrane properties and the actions of dopamine and opioids** *J Neurosci* **9**:1233–1241 https://doi.org/10.1523/JNEUROSCI.09-04-01233.1989

Latif S. *et al.* (2021) **Dopamine in Parkinson's disease** *Clin Chim Acta* **522**:114–126 https://doi.org/10.1016/j.cca.2021.08.009

Lebestky T., Chang J. S., Dankert H., Zelnik L., Kim Y. C., Han K. A., Wolf F. W., Perona P., Anderson D. J (2009) **Two different forms of arousal in Drosophila are oppositely regulated by the dopamine D1 receptor ortholog DopR via distinct neural circuits** *Neuron* **64**:522–536 https://doi.org/10.1016/j.neuron.2009.09.031

Lerner T. N., Holloway A. L., Seiler J. L (2021) **Dopamine, Updated: Reward Prediction Error and Beyond** *Curr Opin Neurobiol* **67**:123–130 https://doi.org/10.1016/j.conb.2020.10.012

Lima S. Q., Miesenbock G (2005) **Remote control of behavior through genetically targeted photostimulation of neurons** *Cell* **121**:141–152 https://doi.org/10.1016/j.cell.2005.02.004

Lippert R. N., Hess S., Klemm P., Burgeno L. M., Jahans-Price T., Walton M. E., Kloppenburg P., Bruning J. C (2020) **Maternal high-fat diet during lactation reprograms the dopaminergic circuitry in mice** *J Clin Invest* **130**:3761–3776 https://doi.org/10.1172/JCI134412

Liu C., Goel P., Kaeser P. S (2021) **Spatial and temporal scales of dopamine transmission** *Nat Rev Neurosci* **22**:345–358 https://doi.org/10.1038/s41583-021-00455-7

Liu C., Xue Y., Liu M. F., Wang Y., Liu Z. R., Diao H. L., Chen L (2018) **Orexins increase the firing activity of nigral dopaminergic neurons and participate in motor control in rats** *J Neurochem* **147**:380–394 https://doi.org/10.1111/jnc.14568

Mahler S. V., Moorman D. E., Smith R. J., James M. H., Aston-Jones G (2014) **Motivational activation: a unifying hypothesis of orexin/hypocretin function** *Nat Neurosci* **17**:1298–1303 https://doi.org/10.1038/nn.3810

Mahler S. V., Smith R. J., Moorman D. E., Sartor G. C., Aston-Jones G (2012) **Multiple roles for orexin/hypocretin in addiction** *Prog Brain Res* **198**:79–121 https://doi.org/10.1016/B978-0-444-59489-1.00007-0

Marcus J. N., Aschkenasi C. J., Lee C. E., Chemelli R. M., Saper C. B., Yanagisawa M., Elmquist J. K (2001) **Differential expression of orexin receptors 1 and 2 in the rat brain** *J Comp Neurol* **435**:6–25 https://doi.org/10.1002/cne.1190

Nair-Roberts R. G., Chatelain-Badie S. D., Benson E., White-Cooper H., Bolam J. P., Ungless M. A (2008) **Stereological estimates of dopaminergic, GABAergic and glutamatergic neurons in the ventral tegmental area, substantia nigra and retrorubral field in the rat** *Neuroscience* **152**:1024–1031 https://doi.org/10.1016/j.neuroscience.2008.01.046

Nakamura T., Uramura K., Nambu T., Yada T., Goto K., Yanagisawa M., Sakurai T (2000) **Orexin-induced hyperlocomotion and stereotypy are mediated by the dopaminergic system** *Brain Res* **873**:181–187 https://doi.org/10.1016/s0006-8993(00)02555-5

Narayanan N. S., Guarnieri D. J., DiLeone R. J (2010) **Metabolic hormones, dopamine circuits, and feeding** *Front Neuroendocrinol* **31**:104–112 https://doi.org/10.1016/j.yfrne.2009.10.004

Neuhoff H., Neu A., Liss B., Roeper J (2002) **I(h) channels contribute to the different functional properties of identified dopaminergic subpopulations in the midbrain** *J Neurosci* **22**:1290–1302 https://doi.org/10.1523/JNEUROSCI.22-04-01290.2002

Palmiter R. D (2007) **Is dopamine a physiologically relevant mediator of feeding behavior?** *Trends in Neurosciences* **30**:375–381 https://doi.org/10.1016/j.tins.2007.06.004

Paxinos G., Franklin K. B. J., Franklin K. B. J (2013) **Paxinos and Franklin's the mouse brain in stereotaxic coordinates (4th ed.)**

Peyron C., Tighe D. K., van den Pol A. N., de Lecea L., Heller H. C., Sutcliffe J. G., Kilduff T. S. (1998) **Neurons containing hypocretin (orexin) project to multiple neuronal systems** *J Neurosci* **18**:9996–10015 https://doi.org/10.1523/JNEUROSCI.18-23-09996.1998

Richards C. D., Shiroyama T., Kitai S. T (1997) **Electrophysiological and immunocytochemical characterization of GABA and dopamine neurons in the substantia nigra of the rat** *Neuroscience* **80**:545–557 https://doi.org/10.1016/s0306-4522(97)00093-6

Roeper J (2013) **Dissecting the diversity of midbrain dopamine neurons** *Trends in Neurosciences* **36**:336–342 https://doi.org/10.1016/j.tins.2013.03.003

Roseberry T. K., Lee A. M., Lalive A. L., Wilbrecht L., Bonci A., Kreitzer A. C (2016) **Cell-Type-Specific Control of Brainstem Locomotor Circuits by Basal Ganglia** *Cell* **164**:526–537 https://doi.org/10.1016/j.cell.2015.12.037

Ruud J. *et al.* (2019) **The fat mass and obesity-associated protein (FTO) regulates locomotor responses to novelty via D2R medium spiny neurons** *Cell Rep* **27**:3182–3198 https://doi.org/10.1016/j.celrep.2019.05.037

Sakurai T. *et al.* (1998) **Orexins and orexin receptors: a family of hypothalamic neuropeptides and G protein-coupled receptors that regulate feeding behavior** *Cell* **92**:573–585 https://doi.org/10.1016/S0092-8674(00)80949-6

Sharples S. A., Koblinger K., Humphreys J. M., Whelan P. J (2014) **Dopamine: a parallel pathway for the modulation of spinal locomotor networks** *Front Neural Circuits* **8** https://doi.org/10.3389/fncir.2014.00055

Soya S., Sakurai T (2020) **Evolution of orexin neuropeptide system: structure and function** *Front Neurosci* **14** https://doi.org/10.3389/fnins.2020.00691

Takatoh J., Nelson A., Zhou X., Bolton M. M., Ehlers M. D., Arenkiel B. R., Mooney R., Wang F (2013) **New modules are added to vibrissal premotor circuitry with the emergence of exploratory whisking** *Neuron* **77**:346–360 https://doi.org/10.1016/j.neuron.2012.11.010

Tsujino N., Sakurai T (2013) **Role of orexin in modulating arousal, feeding, and motivation** *Front Behav Neurosci* **7** https://doi.org/10.3389/fnbeh.2013.00028

Tung L. W. *et al.* (2016) **Orexins contribute to restraint stress-induced cocaine relapse by endocannabinoid-mediated disinhibition of dopaminergic neurons** *Nat Commun* **7** https://doi.org/10.1038/ncomms12199

Turiault M., Parnaudeau S., Milet A., Parlato R., Rouzeau J. D., Lazar M., Tronche F (2007) **Analysis of dopamine transporter gene expression pattern --generation of DAT-iCre transgenic mice** *FEBS J* **274**:3568–3577 https://doi.org/10.1111/j.1742-4658.2007.05886.x

Volkow N. D., Swanson J. M (2013) **Clinical practice: Adult attention deficit-hyperactivity disorder** *N Engl J Med* **369**:1935–1944 https://doi.org/10.1056/NEJMcp1212625

Wang G. J., Volkow N. D., Logan J., Pappas N. R., Wong C. T., Zhu W., Netusil N., Fowler J. S (2001) **Brain dopamine and obesity** *Lancet* **357**:354–357 https://doi.org/10.1016/s0140-6736(00)03643-6

Xiao X. *et al.* (2021) **Orexin receptors 1 and 2 in serotonergic neurons differentially regulate peripheral glucose metabolism in obesity** *Nature Communications* **12** https://doi.org/10.1038/s41467-021-25380-2

Zachry J. E., Nolan S. O., Brady L. J., Kelly S. J., Siciliano C. A., Calipari E. S (2021) **Sex differences in dopamine release regulation in the striatum** *Neuropsychopharmacology* **46**:491–499 https://doi.org/10.1038/s41386-020-00915-1

Zych S. M., Ford C. P (2022) **Divergent properties and independent regulation of striatal dopamine and GABA co-transmission** *Cell Rep* **39** https://doi.org/10.1016/j.celrep.2022.110823

Editors

Reviewing Editor
Laura Bradfield
University of Technology Sydney, Sydney, Australia

Senior Editor
Kate Wassum
University of California, Los Angeles, Los Angeles, United States of America

Reviewer #1 (Public review):

In this manuscript, the role of orexin receptors in dopamine transmission is studied. It extends previous findings suggesting an interplay of these two systems in regulating behaviour by first characterising the expression of orexin receptors in the midbrain and then disrupting orexin transmission in dopaminergic neurons by deleting its predominant receptor, OX1R (Ox1R fl/fl, Dat-Cre tg/wt mice). Electrophysiological and calcium imaging data suggest that orexin A acutely and directly stimulates SN and VTA dopaminergic neurons, but does not seem to induce c-Fos expression. Behavioural effects of depleting OX1R from dopaminergic neurons includes enhanced novelty-induced locomotion and exploration, relative to littermate controls (Ox1R fl/fl, Dat-Cre wt/wt). However, no difference between groups is observed in tests that measure reward processing, anxiety, and energy homeostasis.

To test whether depletion of OX1R alters overall orexin-triggered activation across the brain, PET imaging is used in OX1RΔDAT knockout and control mice. This analysis reveals that several regions show a higher neuronal activation after orexin injection in OX1RΔDAT mice, but the authors focus their follow up study on the dorsal bed nucleus of the stria terminalis (BNST) and lateral paragigantocellular nucleus (LPGi). Dopaminergic inputs and expression of dopamine receptors type-1 and -2 (DRD1 & DRD2) is assessed and compared to control demonstrating moderate decrease of DRD1 and DRD2 expression in BNST of OX1RΔDAT mice and unaltered expression of DRD2, with absence of DRD1 expression in LPGi of both groups. Overall, this study is valuable for the information it provides on orexin receptor expression and function on behaviour and for the new tools it generated for the specific study of this receptor in dopaminergic circuits.

Strengths:

The use of a transgenic line that lacks OX1R in dopamine-transporter expressing neurons is a strong approach to dissect the direct role of orexin in modulating dopamine signalling in the brain. The battery of behavioural assays to study this line provides a valuable source of information for researchers interested in the role of orexin in animal physiology.

Weaknesses:

This study falls short in providing evidence for an anatomical substrate of the altered behaviour observed in mice lacking orexin receptor subtype 1 in dopaminergic neurons. How orexin transmission in dopaminergic neurons regulates the expression of postsynaptic dopamine receptors (as observed in BNST of OX1RΔDAT mice) is an intriguing question poorly discussed. Whether disruption of orexin activity alters dopamine release in target areas is an important point not addressed.

https://doi.org/10.7554/eLife.91716.2.sa2

Reviewer #2 (Public review):

Summary:

This manuscript examines expression of orexin receptors in midbrain - with a focus on dopamine neurons - and uses several fairly sophisticated manipulation techniques to explore the role of this peptide neurotransmitter in reward-related behaviors. Specifically, in situ hybridization is used to show that dopamine neurons predominantly express orexin receptor 1 subtype and then go on to delete this receptor in dopamine transporter-expressing using a transgenic strategy. Ex vivo calcium imaging of midbrain neurons is used to show that, in the absence of this receptor, orexin is no longer able to excite dopamine neurons of the substantia nigra.

The authors proceed to use this same model to study the effect of orexin receptor 1 deletion on a series of behavioral tests, namely, novelty-induced locomotion and exploration, anxiety-related behavior, preference for sweet solutions, cocaine-induced conditioned place preference, and energy metabolism. Of these, the most consistent effects are seen in the tests of novelty-induced locomotion and exploration in which the mice with orexin 1 receptor deletion are observed to show greater levels of exploration, relative to wild-type, when placed in a novel environment, an effect that is augmented after icv administration of orexin.

In the final part of the paper, the authors use PET imaging to compare brain-wide activity patterns in the mutant mice compared to wildtype. They find differences in several areas both under control conditions (i.e., after injection of saline) as well as after injection of orexin. They focus in on changes in dorsal bed nucleus of stria terminalis (dBNST) and the lateral paragigantocellular nucleus (LPGi) and perform analysis of the dopaminergic

projections to these areas. They provide anatomical evidence that these regions are innervated by dopamine fibers from midbrain, are activated by orexin in control, but not mutant mice, and that dopamine receptors are present. Thus, they argue these anatomical data support the hypothesis that behavioral effects of orexin receptor 1 deletion in dopamine neurons are due to changes in dopamine signaling in these areas.

Strengths:

Understanding how orexin interacts with the dopamine system is an important question and this paper contains several novel findings along these lines. Specifically:

(1) Distribution of orexin receptor subtypes in VTA and SN is explored thoroughly.
(2) Use of the genetic model that knocks out a specific orexin receptor subtype from dopamine-transporter-expressing neurons is a useful model and helps to narrow down the behavioral significance of this interaction.
(3) PET studies showing how central administration of orexin evokes dopamine release across the brain is intriguing, especially that two key areas are pursued - BNST and LPGi - where the dopamine projection is not as well described/understood.

Weaknesses:

The role of the orexin-dopamine interaction is not explored in enough detail. The manuscript presents several related findings, but the combination of anatomy and manipulation studies do not quite tell a cogent story. Ideally, one would like to see the authors focus on a specific behavioral parameter and show that one of their final target areas (dBNST or LPGi) was responsible or at least correlated with this behavioral readout.

In many places in the Results, insufficient explanation and statistical reporting is provided. Throughout the Results - especially in the section on behavior although not restricted to this part - statements are made without statistical tests presented to back up the claims, e.g., "Compared to controls, Ox1RΔDAT 143 mice did not show significant changes in spontaneous locomotor activity in home cages" (L143) and "In a hole-board test, female Ox1RΔDAT mice showed increased nose pokes into the holes in early (1st and 2nd) sessions compared to control mice" (L151). In other places, ANOVAs are mentioned but full results including main effects and interactions are not described in detail, e.g., in F3-S3, only a single p-value is presented and it is difficult to know if this is the interaction term or a post hoc test (L205). These and all other statements need statistics included in the text as support. Addition of these statistical details was also requested by the editor.

In the presentation of reward processing this is particularly important as no statistical tests are shown to demonstrate that controls show a cocaine-induced preference or a sucrose preference. Here, one option would be to perform one-sample t-tests showing that the data were different to zero (no preference). As it is, the claim that "Both of the control and Ox1RΔDAT groups showed a preference for cocaine injection" is not yet statistically supported.

https://doi.org/10.7554/eLife.91716.2.sa1

Author response:

The following is the authors' response to the original reviews.

> ***Public Reviews:***

> ***Reviewer #1 (Public Review):***
>
> *Summary:*
>
> *In this manuscript, the role of orexin receptors in dopamine neurons is studied. Considering the importance of both orexin and dopamine signalling in the brain, with critical roles in arousal and drug seeking, this study is important to understand the anatomical and functional interaction between these two neuromodulators. This work suggests that such interaction is direct and occurs at the level of SN and VTA, via the expression of OX1R-type orexin receptors by dopaminergic neurons.*
>
> *Strengths:*
>
> *The use of a transgenic line that lacks OX1R in dopamine-transporter-expressing neurons is a strong approach to dissecting the direct role of orexin in modulating dopamine signalling in the brain. The battery of behavioural assays to study this line provides a valuable source of information for researchers interested in the role of orexin-A in animal physiology.*

We thank the reviewer for summarizing the importance and significance of our study.

> *Weaknesses:*
>
> *The choice of methods to demonstrate the role of orexin in the activation of dopamine neurons is not justified and the quantification methods are not described with enough detail. The representation of results can be dramatically improved and the data can be statistically analysed with more appropriate methods.*

We have further improved our description of the methods in the revised reviewed preprint, and here in the response letter, we respond point-by-point to 'Reviewer #1 (Recommendations For The Authors)' below.

> ***Reviewer #2 (Public Review):***
>
> *Summary:*
>
> *This manuscript examines the expression of orexin receptors in the midbrain - with a focus on dopamine neurons - and uses several fairly sophisticated manipulation techniques to explore the role of this peptide neurotransmitter in reward-related behaviors. Specifically, in situ hybridization is used to show that dopamine neurons predominantly express the orexin receptor 1 subtype and then go on to delete this receptor in dopamine neurons using a transgenic strategy. Ex vivo calcium imaging of midbrain neurons is used to show that in the absence of this receptor orexin is no longer able to excite dopamine neurons of the substantia nigra.*
>
> *The authors proceed to use this same model to study the effect of orexin receptor 1 deletion on a series of behavioral tests, namely, novelty-induced locomotion and exploration, anxiety-related behavior, preference for sweet solutions, cocaine-induced conditioned place preference, and energy metabolism. Of these, the most consistent effects are seen in the tests of novelty-induced locomotion and exploration in which the mice with orexin 1 receptor deletion are observed to show greater levels of exploration, relative to wild-type, when placed in a novel environment, an effect that is augmented after icv administration of orexin.*
>
> *In the final part of the paper, the authors use PET imaging to compare brain-wide activity patterns in the mutant mice compared to wildtype. They find differences in*

> *several areas both under control conditions (i.e., after injection of saline) as well as after injection of orexin. They focus on changes in the dorsal bed nucleus of stria terminalis (dBNST) and the lateral paragigantocellular nucleus (LPGi) and perform analysis of the dopaminergic projections to these areas. They provide anatomical evidence that these regions are innervated by dopamine fibers from the midbrain, are activated by orexin in control, but not mutant mice, and that dopamine receptors are present. Thus, they argue these anatomical data support the hypothesis that behavioral effects of orexin receptor 1 deletion in dopamine neurons are due to changes in dopamine signaling in these areas.*
>
> *Strengths:*
>
> *Understanding how orexin interacts with the dopamine system is an important question and this paper contains several novel findings along these lines. Specifically:*
>
> *(1) The distribution of orexin receptor subtypes in VTA and SN is explored thoroughly.*
>
> *(2) Use of the genetic model that knocks out a specific orexin receptor subtype from only dopamine neurons is a useful model and helps to narrow down the behavioral significance of this interaction.*
>
> *(3) PET studies showing how central administration of orexin evokes dopamine release across the brain is intriguing, especially since two key areas are pursued - BNST and LPGi - where the dopamine projection is not as well described/understood.*

We thank the reviewer for the careful summary and highlighting the novelty of our study.

> *Weaknesses:*
>
> *The role of the orexin-dopamine interaction is not explored in enough detail. The manuscript presents several related findings, but the combination of anatomy and manipulation studies does not quite tell a cogent story. Ideally, one would like to see the authors focus on a specific behavioral parameter and show that one of their final target areas (dBNST or LPGi) was responsible or at least correlated with this behavioral readout. In addition, some more discussion on what the results tell us about orexin signaling to dopamine neurons under normal physiological conditions would be very useful. For example, what is the relevance of the orexin-dopamine interaction blunting noveltyinduced locomotion under wildtype conditions?*

We agree that focusing on some orexin-dopamine targeting areas, such as dBNST or LPGi, is important to further reveal the anatomy-behavior links and underlying mechanisms. While we are very interested in further investigations, in the present manuscript we mainly aim to give an overview of the behavioral roles of orexin-dopamine interaction and to propose some promising downstream pathways in a relatively broad and systematical way.

We have explained the physiological meanings of our results in more detail in the discussion in the revised reviewed preprint (lines 282-293, 318-332,). Novelty-induced behavioral response should be at proper levels under normal physiological conditions. The orexin-dopamine interaction blunting novelty-induced locomotion could be important to keep attention on the main task without being distracted too much by other random stimuli in the environment. When this balance is disrupted, behavioral deficit may happen, such as attention deficit and hyperactivity disorder (ADHD).

> *In some places in the Results, insufficient explanation and reporting is provided. For example, when reporting the behavioral effects of the Ox1 deletion in two bottle preference, it is stated that "[mutant] mice showed significant changes..." without stating the direction in which preference was affected.*

For the reward-related behaviors described in this study, we did not find significant changes between [mutant] and control mice. We agree that it will be helpful for readers by describing the behavioral tests in more details. In the revised reviewed preprint, we have described in more detail in the results and Materials and Methods section how the control and [mutant] mice behave to the reward (lines 162-165, 171-181, 526-528).

> *The cocaine CPP results are difficult to interpret because it is unclear whether any of the control mice developed a CPP preference. Therefore, it is difficult to conclude that the knockout animals were unaffected by drug reward learning. Similarly, the sucrose/sucralose preference scores are also difficult to interpret because no test of preference vs. water is performed (although the data appear to show that there is a preference at least at higher concentrations, it has not been tested).*

We described the CPP analysis in the Materials and Methods section (lines 523-528) as below: 'The percentage of time spent in the reward-paired compartment was calculated: 100 x time spent in the compartment / (total time - time spent in the middle area). The CPP score was then analyzed using the calculated percentage of time: 100 x (time on the test day – time on pre-test days)/ time on pre-test days. The pre-test and test days were before and after the conditioning, respectively. Thus, the CPP score above zero indicates that the CPP preference has developed.' In Figure 2—figure supplement 4 C and F, it was shown that most control and knockout mice had a CPP score above zero. The control and knockout groups both developed a preference and there was no significant difference between the groups.

For the sucrose/sucralose preference tests, in Figure 2—figure supplement 4 A and D, we present values as the percentages of sucrose/sucralose consumption in total daily drinking amount (sucrose/sucralose solution + water). Thus, percentages above 50% indicates mice prefer sucrose/sucralose to water. As shown in the figure, male mice only showed weak preference of 0.5% sucrose, compared to water, and under all other tested conditions, the mice showed strong preference of the sweet solution. There was no significant difference between control and knockout mice.

We have described this in more details in the Results and Materials and Methods section in the revised reviewed preprint.

> ***Recommendations for the authors:***
>
> ***Reviewer #1 (Recommendations For The Authors):***
>
> *(1) Figure 1, A-I. It is difficult to depict the anatomical subdivision of VTA in Figure 1, panels A and B. It is recommended to add a panel showing a schematic illustration of the SNc and subregions of VTA: PN, PIF, PBP, IF (providing more detail than in Figure 1, panel J). It is also recommended to show lower magnification images (as in Figure 1 - supplement 1), including both hemispheres, and to delineate the outline of the different subregions using curved lines, based on reference atlases (similar to Figure 1, panel I, please include distance from bregma). It would be helpful to indicate in Figure 1 that panel A is a control mouse and panel B is a Ox1RΔDAT mouse and include C-F letters to show corresponding insets. Anatomically, the paraintrafasicular nucleus (PIF) is positioned between the paranigral nucleus (PN) and the parabrachial pigmented nucleus (PBP). The authors have depicted the PIF ventral to the PN in Figure 1 panels A, B, and I. These panels and the quantification of Ox1R/2R positive cells within the different subdivisions need to be corrected accordingly. The image analysis method used to quantify RNAscope fluorescent images is not described in sufficient detail. Please expand this section.*

According to the reviewer's suggestions, we have refined Figure 1 in the revised reviewed preprint. We are now showing the schematic illustration of the SN and subregions of VTA in panel I, with blue squares to label the regions shown in panels A and B, and the distance from bregma is included. The outlines to delineate SN and the subregions of VTA are adjusted from straight to curved lines based on reference atlases. As suggested, we have also indicated panel A is a control and panel B is a Ox1RΔDAT mouse and included C-F letters to show corresponding insets. We apologize for the mistake about labeling PIF and PN positions in Figure A. We have corrected the labeling of their positions and double checked the quantification accordingly. This does not change our discussion or conclusion since both PIF and PN are the medial part of VTA, where both Ox1R and Ox2R are observed. The description of the image analysis in Matierials and Methods section has been improved (lines 378-385). We decided not to show lower magnification images than in Figure 1—supplement 1 to include both hemispheres, in the interests of clarity and reader-friendliness.

> *(2) Figure 1, J-L. The claim that orexin activates dopaminergic SN and VTA neurons is weakly supported by the data provided. Calcium imaging of SN dopaminergic neurons in control mice suggests a discrete effect of 100 nM orexin-A application compared to baseline. Application of 300 nM shows a slightly bigger effect, but none of these results are statistically analysed.*

We are surprised by this comment and thank the reviewer for pointing out our apparent lack of clarity in the previous version (lines 96-106 and legend of Figure 1K, L). In more detail, we explain the data analysis in the new version (lines 119-133, 451-465) and the legend of Figure 1K, L and Figure 1-figure supplement 3).

The main goal of this part of the project was to functionally validate the Ox1R knockout in dopaminergic (DAT-expressing) neurons. This was a prerequisite for the behavioral and PET imaging experiments. We used GCaMP-mediated Ca2+ imaging in acute brain slices to reach this goal. This analysis was performed on the dopaminergic SN neurons, which we used as an "indicator population" because a large number of these neurons express Ox1R, but only a few express Ox2R.

The analysis consisted of two parts:

a) For each neuron, we tested whether it responded to orexin A. At the single cell level, a neuron was considered orexin A-responsive if the change in fluorescence induced by orexin A was three times larger than the standard deviation (3 σ criterion) of the baseline fluorescence, corresponding to a Zscore of 3. We found that 56% of the neurons tested responded to orexin A, while 44% of the neurons did not respond to orexin A (Figure 1L, top). These data agree with the number of Ox1R-expressing neurons (Figure 1J).

b) We also determined the orexin A-induced GCaMP fluorescence for each neuron, expressed as a percentage of GCaMP fluorescence induced upon application of high K+ saline. Accordingly, the "population response" of all analyzed neurons was expressed as the mean ± SEM of these responses. The significance of this mean response was tested for each group (control and Ox1R KO) using a onesample t-test. We found a marked and highly significant ($p < 0.0001$, $n = 71$) response of control neurons to 100 nM orexin A, while the Ox1R KO neurons did not respond ($p = 0.5$, $n = 86$). Note that, as described in a), 44% of the neurons contributing to the mean do not respond to orexin. Thus, the orexin responses of most responders are significantly higher than the mean. This is also evident in the example recordings in Figure 1K and Figure1—figure supplement 3. The orexin A-induced change in fluorescence was increased by increasing the orexin A concentration to 300 nM.

Note: As mentioned above, the orexin A response was expressed for each neuron individually as a percentage of its high K+saline-induced GCaMP fluorescence. This value is a solid

reference point, reflecting the GCaMP fluorescence at maximal voltage-activated Ca2+ influx. Obviously, the Ca2+ concentration at this point is extremely high and not typically reached under physiological conditions. Therefore, as shown in Figure1—figure supplement 3 for completeness, the physiologically relevant responses may appear relatively minor at first glance when presented together in one figure (compare Figure1—figure supplement 3 A and B).

> *The authors should provide more evidence of the orexin-induced activation of dopaminergic neurons in the SN to support this claim and investigate whether a similar activation is observed in VTA neurons.*

Following the reviewer's suggestion, we confirmed orexin A-induced activation of dopaminergic neurons in the mouse SN by using perforated patch clamp recordings (Figure1—figure supplement 2).

This finding is consistent with previous extracellular in vivo recordings in rats (Liu et al., 2018).

The activation of dopaminergic neurons in the mouse VTA by orexin A has been shown repeatedly in earlier studies (e.g., Baimel et al., 2017; Korotkova et al., 2003; Tung et al., 2016).

> *In addition, Figure 3-Figure Supplement 2 shows that injection of orexin does not induce c-Fos expression in SN and VTA dopaminergic neurons of control and Ox1RΔDAT mice, which further weakens the claim made by the authors.*

Figure 3—Figure Supplement 2 in the original submission is now Figure 3—Figure Supplement 3 in the revised reviewed preprint. It shows low c-Fos expression in SN and VTA dopaminergic neurons, and orexin-induced c-Fos expression was observed in Th-negative cells in SN and VTA.

Technically relatively straightforward, Fos analysis is widely (and successfully) used in studies to reveal neuronal activation. However, this approach has limitations, e.g., regarding sensitivity and temporal resolution. Electrophysiological or optical imaging techniques can circumvent these shortcomings. The electrophysiological and Ca2+ imaging studies presented here, along with previous electrophysiological studies by others, clearly show that orexin A acutely and directly stimulates SN and VTA dopaminergic neurons.

In vivo, the injection of orexin A induced a pronounced c-Fos activity in non-dopaminergic cells of the VTA and SN but not in dopaminergic neurons. This result shows that the detection of c-Fos has worked in principle. Whether the absent c-Fos staining in dopaminergic neurons is due to lack of sensitivity, whether other IEGs would have worked better here, or whether there are other, e.g., cell type-specific reasons for the absence of staining, cannot be determined from the current data.

> *(3) Figure 2, I-L. The fact that ICV injection of both saline and orexin causes a sustained increase of locomotion (around 20 minutes in males, and over 30 minutes in females) is problematic and could mask the effects of orexin, particularly in females. It is unclear what panels J and L are showing. To be appropriately analysed, the authors should plot the pre- and post-injection AUC data for all groups and analyse it as a two-way mixed ANOVA, with the within-subjects factor "pre/post injection activity" and between-subjects factor "group". The authors can only warrant a statistically meaningful hyperlocomotor effect in Ox1RΔDAT mice if a significant interaction is found.*

Though mice were habituated to the injection, it still makes sense to see the injection-induced increase in locomotion to some extent. We described in the figure legend that the AUC was

calculated for the period after orexin injection, which meant 5 – 90 min in Figure 2 I, K. We have clearly observed significant differences between genotypes and between saline and orexin application, which means the genotype and orexin impact is strong enough to pop up despite of the injection effect.

As the reviewer's suggests, we have now plotted the pre- and post-injection AUC data for all groups and analyzed it as a two-way mixed ANOVA, with the within-subjects factor "pre/post injection activity" and between-subjects factor "group". To match the pre- and post-injection duration, we are now comparing AUC for around 60 min before and after the injection. A significant interaction is found here. Panels I-L are renewed, and the differences induced by Ox1R knockout and orexin confirmed the results shown in the initially submitted manuscript.

> *(4) Figure 3. The literature has robustly shown that one of the main projection areas of VTA and SN dopaminergic neurons is the striatum, in particular its ventral part. It is surprising to see that this region is not affected by the lack of OX1R or by the injection of orexin. How can the authors explain that identified regions with significantly different activity include neighbouring brain structures with heterogenous composition? See for example, in panel A, section bregma 0.62mm, a significant region is seen expanding across the cortex, corpus callosum, and striatum. While the data from PET studies is potentially interesting, it may not be adequate to provide enough resolution to allow examination of the anatomical distribution of orexin-mediated neuronal activation.*

While the striatum is a major projection area of dopaminergic neurons in VTA and SN, the projection and function of Ox1R-positive dopaminergic neurons is not clear. We have improved the description of dopamine function diversity in the revised reviewed preprint (lines 46-58), and it was reported before that the projection-defined dopaminergic populations in the VTA exhibited different responses to orexin A (Baimel et al., 2017). Moreover, the striatum activity is modulated by the indirect effect via other brain regions affected by Ox1R-positive dopaminergic neurons. It is unknown how the striatum activity should change after Ox1R deletion in dopaminergic neurons. We could not rule out the possibility that the striatum is indeed modulated by the Ox1R-positive dopaminergic neurons, though there was only a trend of genotype difference (Ox1RΔDAT vs. ctrl) in the ventral striatum in the section bregma 1.42 mm in Figure 3A. The ICV injection of orexin is potentially acting on Ox1R and Ox2R in the whole brain, so projections from other brain regions to the striatum also affect striatum activity and could have masked the effect of Ox1R-positive dopaminergic neurons.

The spatial resolution of the PET data is in the order of ~1 mm^3. As we also explained in the Materials and Methods section, the size of a voxel in the original PET data is 0.4mm x 0.4mm x 0.8 mm. All calculations were performed on this grid. The higher-resolved images shown in Figure 3 are for presentation purposes only inspired by a request of the reviewer who asked us to show this in the Jais et al. 2016 manuscript. To make this clearer we now added the p-map images with the original voxel size to the supplement (Figure 3—figure supplement 1). For the interest in specific brain areas, more precise identification of anatomical sub-regions requires using methods with higher spatial resolution such as staining of brain slices for c-Fos-positive cells as we do in Figure 4.

PET is a powerful tool to identify global regions of activation/inhibition. In the manuscript, we have described in the results and discussion section that the activity in brain regions with related functions were changed. In panel A, Ox1RΔDAT showed activity increase in MPA, Pir and endopiriform claustrum, which are important for olfactory sensation; spinal trigeminal nucleus, sp5, and IRt, which regulates mastication and sensation of the oral cavity and the surface of the face; SubCV and Gi, which regulates sleeping and motion-related arousal and motivation. In panel B, changes in HDB, MCPO, Pir, DEn, S1, V2L and V1 are related to

sensation, and changes in BNST, LPGi and M2 are important for emotion, exploration, and action selection.

> *(5) Figure 4. As in Figure 1, the authors should consider including a schematic illustration of the brain areas that are being analysed using a reference atlas. It is also recommended to provide more details describing the quantification of the images. Without such information, the data is not convincing, in particular, the claim that Ox1R depletion causes a decrease in DRD1 in BNST is unclear. Additional unbiased quantitative approaches could be used to strengthen this point.*

We have added Figure 4—figure supplement 1 as a schematic illustration of the brain areas that were being analyzed using a reference atlas. More details describing the unbiased quantification of the images have been added to Materials and Methods. We have added Figure 4—figure supplement 3, to show DRD1, DRD2 and the merged signal separately.

> *(6) The discussion starts by stating that the main findings of this study are based on RNAscope and optophysiological experiments, however, the latter are not presented anywhere in the manuscript. This sentence (line 192) should be revised. The authors state in line 193 that OX1R is the only orexin receptor in the SN, but they show in Figure 1 that in the SN, 3% of neurons express OX2R and 2% co-express both receptors.*

We thank the reviewer for the input. We have rephrased the beginning of the discussion to clarify the objectives (lines 238 - 246). In doing so, we changed "optophysiological experiments" and "single orexin receptor" (lines 192 and 193 in the original manuscript) to " Ca2+ imaging experiments" and "main subtype of orexin receptors ", respectively. In this context, it should be noted that Ca2+ imaging is considered an optophysiological method - optophysiology generally refers to techniques that combine optical methods with physiological measurements.

> *The results of LPGi and BNST dopamine receptors in control and Ox1RΔDAT mice are poorly discussed. The authors should justify why these two regions were selected for further validation and how these may be related to the behavioural effects found in Ox1RΔDAT regarding exposure to a novel context.*

Ox1RΔDAT mice exhibited increased novelty- and orexin-induced locomotion compared to control mice. After orexin injection, PET imaging shows that the neural activity of BNST and LPGi was lower or higher than in control mice, respectively. We selected BNST and LPGi for further validation because we think their key functional roles in regulating emotion, exploratory behaviors and locomotor speed are related to novelty-induced locomotion. We confirmed changes in neural activity change by c-Fos staining and investigated the expression patterns of dopamine receptors in BNST and LPGi. Our findings suggested that Ox1R deletion in dopaminergic neurons results in the disinhibition of neural activity in LPGi via dopaminergic pathways and the decrease of dopamine-mediated neural activity in BNST. Emotion perception affects the decision of how to respond to the novelty. It is possible that novelty activates the orexin system and Ox1R signaling in dopaminergic neurons promotes emotion perception and inhibits exploration. Of course, further careful investigation is necessary to test this hypothesis in the future experiments. We have improved the rational description and discussion in the

‘Results’ and ‘Discussion’ section in the revised reviewed preprint (lines 210-213, 259-270, 293-308).

> ***Reviewer #2 (Recommendations For The Authors):***
>
> *A major recommendation - if possible - would be to directly show that one or both of the two target areas - dBNST and LPGi - are associated with the behavioral effects caused by the deletion of the orexin receptor 1 in dopamine neurons.*

We completely agree that it would be very valuable to directly show dBNST and LPGi are associated with the behavioral effects caused by the deletion of Ox1R in dopaminergic neurons. While we are very interested in carefully investigating specific orexin-dopamine targeting areas and related neural circuits in the future, in the present manuscript, we mainly aim to give an overview of the behavioral roles of orexin-dopamine interaction and propose some promising downstream pathways.

> *The authors should state if data are corrected for multiple comparisons, e.g., in the PET study of different regions.*

We have included information about the post-hoc tests for all 2-way ANOVA analyses in the submitted manuscript. For the PET study, the p-values in the p-maps were not corrected for multiple comparison, Figure 3—figure supplement 2 shows the raw data of each mouse and the analysis method (t-test). In the revised reviewed preprint, we include the information on the analysis method in the figure legends of Figure 3.

We consider that saline and orexin injections mimic the resting and active state of mice, respectively, and would like to study genotype effect under each condition. Doing 2-way ANOVA takes in count the difference between orexin and saline injection, which could mask the genotype effect under a certain condition. Therefore, we decided to perform t-tests for each condition in Figure 3. While we provide readers with full information in Figure 3—figure supplement 2 with the raw data of each individual mouse, below we present the p-maps after multiple comparisons (Sidak's post hoc test). After multiple comparisons, we could see changes in similar brain regions as in Figure 3, though significant values are reduced by the correction for multiple comparisons, and under orexin-injection condition, we fail to see significantly higher activity around the lateral paragigantocellular nucleus (LPGi), nucleus of the horizontal limb of the diagonal band (HDB) and magnocellular preoptic nucleus (MCPO) in Ox1RΔDAT mice. In order to more precisely identify the anatomical locations, we performed additional experiments to confirm the changes revealed by PET. For example, LPGi is a relatively small region confirmed and identified more precisely by c-Fos immunostaining (Figure 4A, C).

Author response image 1.

PET imaging studies comparing Ox1RΔDAT and control mice, with post-hoc t-test to correct for multiple comparisons. 3D maps of p-values in PET imaging studies comparing Ox1RΔDAT and control mice, after intracerebroventricular (ICV) injection of (A) saline (NS) and (B) orexin A. Control-NS, n = 8; control-orexin, n = 6; Ox1RΔDAT, n = 8. M2, secondary motor cortex; MPA, medial preoptic area; Pir, piriform cortex; IEn, intermediate endopiriform claustrum; DEn, dorsal endopiriform claustrum; VEn, ventral endopiriform claustrum; LSS, lateral stripe of the striatum; BNST, the dorsal bed nucleus of the stria terminalis; S1Sh, primary somatosensory cortex, shoulder region; S1HL, primary somatosensory cortex, hindlimb region; S1BF, primary somatosensory cortex, barrel field; S1Tr, primary somatosensory cortex, trunk region; V1, primary visual cortex; V2L, secondary visual cortex, lateral area; SubCV, subcoeruleus nucleus, ventral part; Gi, gigantocellular reticular nucleus; IRt, intermediate reticular nucleus; sp5, spinal trigeminal tract.

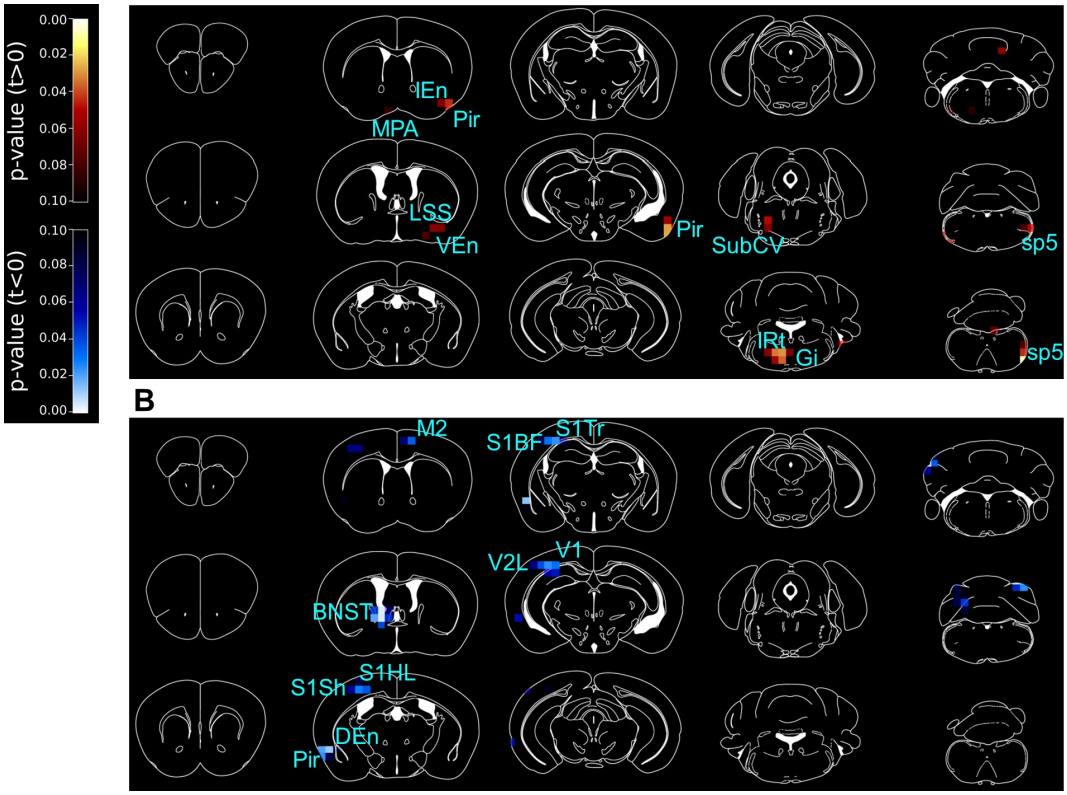

> *Provide a rationale for following up on BNST and LPGi and not any of the regions identified in the PET study.*

We thank the reviewer for the careful reading and important input. Ox1RΔDAT mice exhibited increased novelty- and orexin-induced locomotion compared to control mice. After orexin injection, PET imaging shows that the neural activity of BNST and LPGi was lower or higher than control mice, respectively.

We selected BNST and LPGi for further validation because we think their key functional roles in regulating emotion, exploratory behaviors and locomotor speed are related to novelty-induced locomotion. We confirmed the neural activity change by c-Fos staining and investigated the expression patterns of dopamine receptors in BNST and LPGi. Our findings suggested that Ox1R deletion in dopaminergic neurons results in the disinhibition of neural activity in LPGi via dopaminergic pathways and the decrease of dopamine-mediated neural activity in BNST. Emotion perception affects the decision how to respond to the novelty. It is possible that novelty activates the orexin system and Ox1R signaling in dopaminergic neurons promotes emotion perception and inhibits exploration. Of course, further investigation is necessary to test this hypothesis in future. We have improved the rational description and discussion in the 'Results' and 'Discussion' section in the revised reviewed preprint (lines 210-213, 259-270, 293-308).

> *Heatmap in Fig. 1K should not have smoothing across the y-axis, individual cells should be discrete.*

We thank the reviewer for bringing this issue to our attention. The data had not been intentionally smoothed (neither across the x-axis nor the y-axis), but it was probably a formatting issue. We have corrected this and separated individual cell traces with lines (Figure 1K, Figure 1—figure supplement 3).

> *Dopamine cells are well known to lack Fos expression in most cases. Did the authors consider using another IEG to show neural activation, e.g., pERK?*

We did not use another IEG. The electrophysiological and Ca2+ imaging studies presented here, along with previous electrophysiological studies by others, clearly show that orexin A acutely and directly stimulates SN and VTA dopaminergic neurons. Please see also the response to a related comment of Reviewer 1.

> *Consider adding a lower magnification section to anatomical figures to aid the reader in orienting and identifying the location.*

We have added the schematic illustration of SN, VTA, BNST and LPGi in Figure 1I and Figure 4 — figure supplement 1. We hope this helps the reader in orienting and identifying the location.

> *Data availability should be stated.*

There are no restrictions on data availability. We have added this section to the revised reviewed preprint.

> *Line 50. Some more references both historical and recent could be given to support this statement about the function of dopamine.*

We have improved the description and references to support the statement about dopamine function (lines 46-58). We have cited recent studies and some reviews in the revised reviewed preprint (lines 4658).

> *The PET data (Fig. 3) might be easier to visualize and interpret if a white background was used. In addition, is there a more refined way of presenting the data in Fig 3, S1?*

It is common to present imaging data such as PET and MRI on a black background. We also have already applied this color scheme in multiple publications and would therefore prefer to stick to this color scheme.

While Figure 3 is the concise way to present PET data, we aim to show the original individual results of mice in Figure 3—figure supplement 2 and to demonstrate how we performed the statistical analysis. Therefore, we take an example voxel of the respective brain area, perform the t-test, and present the data as bars with individual dots.

> *Line 97. State what type of Ca imaging here, e.g., "we performed Ca imaging in ex vivo slices of VTA and SN".*

As the reviewer suggested, we have specified the type of Ca2+ imaging (line 112).

> *Line 165. State which groups this post-mortem analysis was performed on and if any differences were to be found (not expected to find differences in this anatomical tracing experiment but good to report this as both groups were used).*

Postmortem analysis of c-Fos staining revealed low c-Fos expression in dopaminergic neurons in the VTA and SN of Ox1RΔDAT and control mice after ICV injection of saline or orexin A (1 nmol). No obvious changes were observed among the groups. We have improved the description in the revised reviewed preprint (lines 202-208).

> *Line 192. What do you mean by optophysiological here? The Ca imaging (which is a fairly small, confirmatory element of the manuscript).*

We have changed 'optophysiological experiments' (line 192 in initial submitted manuscript) to 'calcium imaging experiments' and rephrased the beginning of the discussion to clarify the objectives (lines 238246).

> *The protein level in the diet is substantially higher than in most rodent diets (34% here vs 14-20% in most commercial rodent chows). Please comment on this.*

This diet is for rat and mouse maintenance, purchased from ssniff Spezialdiäten GmbH (product V1554).

The percentage of calories supplied by protein is affected by the calculation methods. The company calculated with pig equation before and the value was 34% in the old instruction data sheet. They have updated the value to 23% in the new data sheet with calculations by Atwater factors. We thank the reviewer for reminding us and have updated the values in the revised reviewed preprint (lines 314-316).

> ***Editor's note:***
>
> *Should you choose to revise your manuscript, please include full statistical reporting including exact p-values wherever possible alongside the summary statistics (test statistic and df) and 95% confidence intervals. These should be reported for all key questions and not only when the p-value is less than 0.05.*

We have provided the source data and the statistical reporting for each Figure with the revision

References

Baimel, C., Lau, B. K., Qiao, M., & Borgland, S. L. (2017). Projection-target-defined effects of orexin and dynorphin on VTA dopamine neurons. *Cell Rep*, *18*(6), 1346-1355. https://doi.org/10.1016/j.celrep.2017.01.030

Korotkova, T. M., Eriksson, K. S., Haas, H. L., & Brown, R. E. (2002). Selective excitation of GABAergic neurons in the substantia nigra of the rat by orexin/hypocretin in vitro. *Regul Pept*, *104*(1-3), 83-89. https://doi.org/10.1016/s0167-0115(01)00323-8

Korotkova, T. M., Sergeeva, O. A., Eriksson, K. S., Haas, H. L., & Brown, R. E. (2003). Excitation of ventral tegmental area dopaminergic and nondopaminergic neurons by orexins/hypocretins. *J Neurosci*, *23*(1), 7-11. https://www.ncbi.nlm.nih.gov/pubmed/12514194

Liu, C., Xue, Y., Liu, M. F., Wang, Y., Liu, Z. R., Diao, H. L., & Chen, L. (2018). Orexins increase the firing activity of nigral dopaminergic neurons and participate in motor control in rats. *J Neurochem*, *147*(3), 380-394. https://doi.org/10.1111/jnc.14568

Tung, L. W., Lu, G. L., Lee, Y. H., Yu, L., Lee, H. J., Leishman, E., Bradshaw, H., Hwang, L. L., Hung, M. S., Mackie, K., Zimmer, A., & Chiou, L. C. (2016). Orexins contribute to restraint stress-induced cocaine relapse by endocannabinoid-mediated disinhibition of dopaminergic neurons. *Nat Commun*, *7*, 12199. https://doi.org/10.1038/ncomms12199

https://doi.org/10.7554/eLife.91716.2.sa0